Introduction to shell-model Monte-Carlo methods

Cem Özen

Gesellschaft für Schwerionenforschung
Darmstadt

Helmholtz International Summer School
Dubna, August 7 - 17, 2007

Motivation and Theoretical Background

Nuclear Landscape

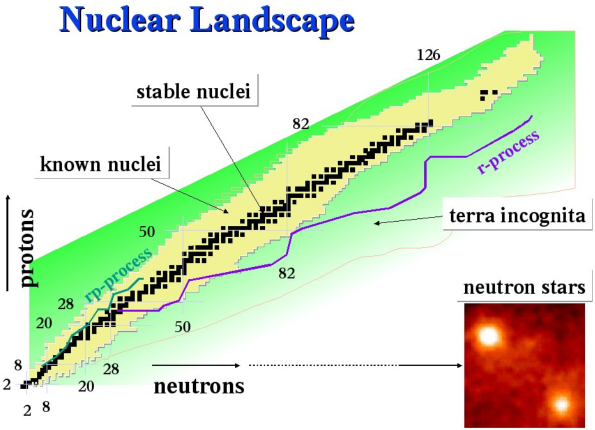

81 stable elements with slightly fewer than 300 stable isotopes
More than 3000 nuclides in total

Methods for Nuclear Many-body Problem

$A = 3$ Solution of Faddeev equation
$A = 4$ Faddeev-Yakubowski method
Up to A=12 Green's Function Monte Carlo (GFMC)
Up to A=16 No-core Shell Model (NCSM)
$A >$16 Many methods exist

Methods for Nuclear Many-body Problem

$A = 3$ Solution of Faddeev equation
$A = 4$ Faddeev-Yakubowski method
Up to A=12 Green's Function Monte Carlo (GFMC)
Up to A=16 No-core Shell Model (NCSM)
$A >$16 Many methods exist
Truncation in model space or correlations needed!

Methods for Nuclear Many-body Problem

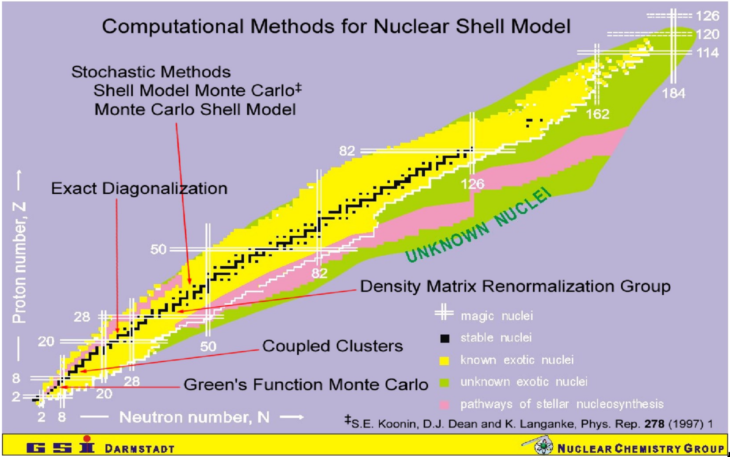

Shell Structure, Valence Space and Residual Interaction

Interacting Shell Model

$$\hat{H} = \hat{H}_0 + \hat{H}_{res} = \sum_i (\hat{t}_i + \hat{U}_i) + \frac{1}{2}\sum_{ij}(\hat{v}_{ij} - 2\hat{U}_i\delta_{ij})$$

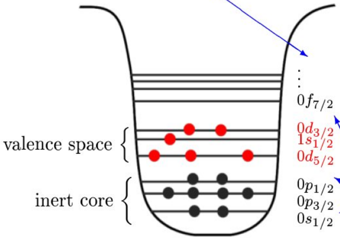

Mean-field potential
Hartree-Fock, Woods-Saxon, Harmonic Oscillator

shell gaps (magic numbers): $2, 8, 20, 28, 50, \ldots$

Shell Structure

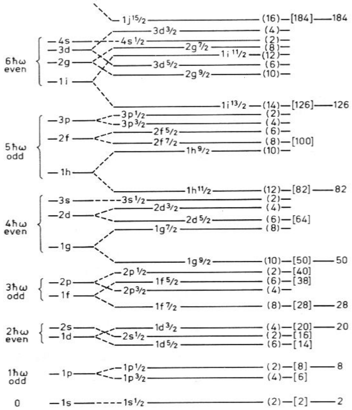

Nuclear shell model is defined by spin-orbit coupled single-particle states:

$$\begin{aligned} |\phi_\alpha\rangle &= |nljmt_z\rangle \\ &= |nl\rangle \otimes |(ls)jm\rangle \otimes |t = \tfrac{1}{2}t_z\rangle \end{aligned}$$

where $j = l + \frac{1}{2}$

and the corresponding single-particle energies ϵ_{nljt_z}

Traditional Shell Model Approach

- Choose a proper model space, i.e. define the valence single-particle states, *e.g.*, for the sd-shell: $1s_{1/2}$, $0d_{5/2}$, $0d_{3/2}$ *orbits.*
- Construct Slater determinants $|\Phi\rangle$ to span the many-body Hilbert space. Often one employs conserved quantities to economize: *M-states, projections (such as J and T etc.)*
- Construct Hamiltonian matrix $H_{i,j} = \langle\Phi_i|H|\Phi_j\rangle$
- Diagonalize the Hamiltonian matrix to find eigenvalues and eigenvectors. *for example, Lanczos algorithm*.

Computational Resources vs. Dimensionalities

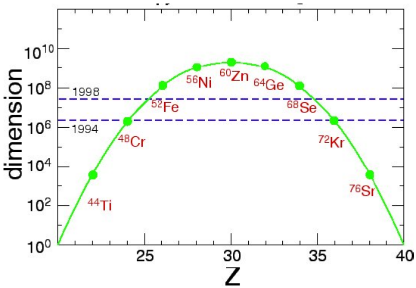

$$D = \binom{N_{sp}}{Z}\binom{N_{sn}}{N}$$

Total # of Slater Det.

$D_m \sim 10^9$ (ANTOINE)

$D_J \sim 10^7$ (NATHAN)

shell	# of single-particle states	nucleus	$M = 0$ states
p	6	^{10}B	84
sd	12	^{28}Si	9.4×10^4
fp	20	^{60}Zn	2.0×10^9

Model Spaces: Progress in Years

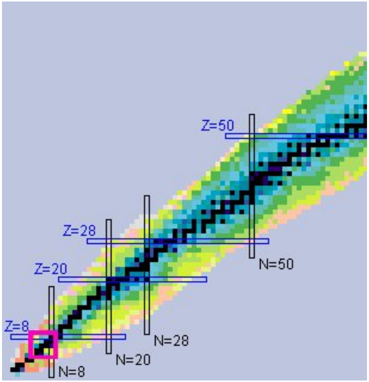

Progress in traditional SM calculations:

p-shell: 10^2 dim. (1960s)

Model Spaces: Progress in Years

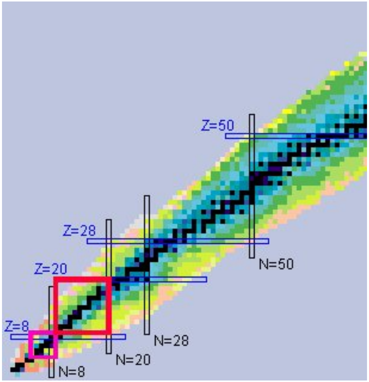

Progress in traditional SM calculations:

p-shell: 10^2 dim. (1960s)
sd-shell 10^5 dim. (1980s)

Model Spaces: Progress in Years

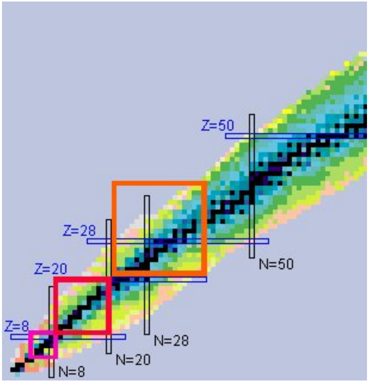

Progress in traditional SM calculations:

p-shell: 10^2 dim. (1960s)
sd-shell 10^5 dim. (1980s)
fp-shell 10^9 dim. (1990s)

Model Spaces: Progress in Years

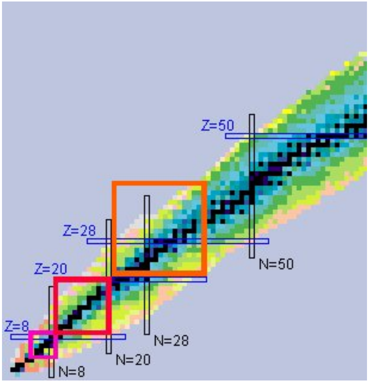

Progress in traditional SM calculations:

p-shell: 10^2 dim. (1960s)
sd-shell 10^5 dim. (1980s)
fp-shell 10^9 dim. (1990s)

Beyond *fp*-shell is far too large for traditional SM!

Model Spaces: Progress in Years

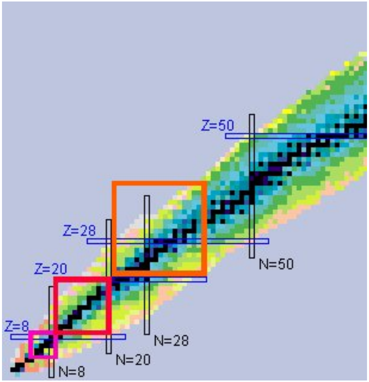

Progress in traditional SM calculations:

p-shell: 10^2 dim. (1960s)
sd-shell 10^5 dim. (1980s)
fp-shell 10^9 dim. (1990s)

Beyond *fp*-shell is far too large for traditional SM!

Compare to recent SMMC calculations:

Model Spaces: Progress in Years

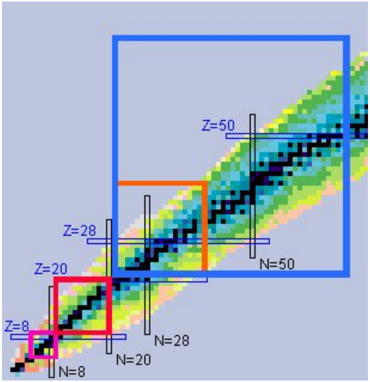

Progress in traditional SM calculations:

p-shell: 10^2 dim. (1960s)
sd-shell 10^5 dim. (1980s)
fp-shell 10^9 dim. (1990s)

Beyond *fp*-shell is far too large for traditional SM!

Compare to recent SMMC calculations:

$fp - gds$-shell 10^{28} dim.

Dimensionalities vs. Computational Power

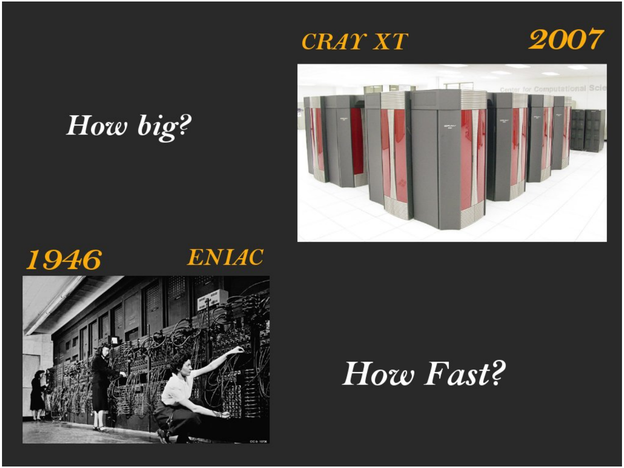

Dimensionalities vs. Computational Power

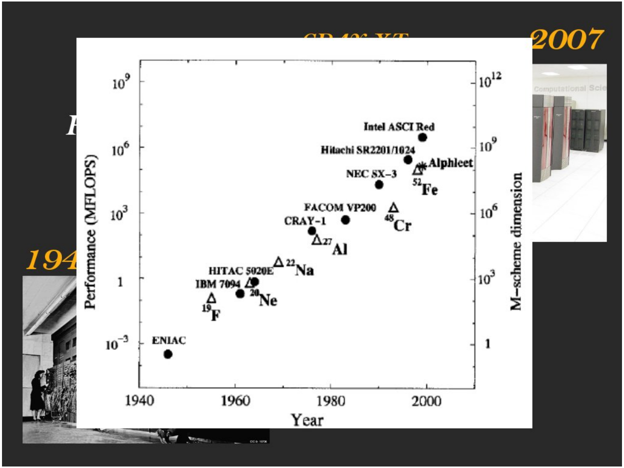

SMMC as an Alternative

- Canonical averages of observables in model spaces that are prohibitively large for direct diagonalization
- Ground state expectation values in the limit of $T \rightarrow 0$
- Thermal and rotational properties of nuclei
- Dynamical response of the system, strength functions
- Well-suited for level density calculations
- Straightforward implementation on parallel machines
- Often one has to deal with sign problem

A Brief History of SMMC

History of SMMC goes back to the pioneering paper:

G. Sugiyama and S. E. Koonin, Ann. Phys. 168, 1 (1986)

Late 90's and early 2000's have seen great progress in nuclear structure calculations particularly for fp-shell nuclei.

[S.E. Koonin, D.J. Dean, K. Langanke, Phys. Rep.**278**, 1 (1997)].

More recently ...

- *Extended the AFMC calculations of level densities to higher temperatures and excitation energies*, Y. Alhassid, G.F. Bertsch and L. Fang, 2003
- *Electron capture rates on nuclei and implications for stellar core collapse*, K. Langanke et. al., 2003
- *SMMC in the pn-formalism*, C. Özen and D. Dean, 2005
- *Implementation of exact spin-projection*, Y. Alhassid, S. Liu and H. Nakada, 2006
- *AFMC applied to thermal properties of nanoparticles*, Y. Alhassid, L. Fang and S. Schmidt, 2007
- *Spin- and parity-resolved level densities*, Y. Kalmykov C. Özen, K. Langanke, G. Martinez-Pinedo, P. von Neumann-Cosel, and A. Richter, 2007.

SMMC in a Nutshell
Motivation

- We would like to calculate:

$$\hat{U} = e^{-\beta \hat{H}} \longrightarrow \langle \hat{X} \rangle = \frac{\mathrm{Tr}[\hat{U}\hat{X}]}{\mathrm{Tr}\hat{U}} \qquad (\beta = \frac{1}{T})$$

SMMC in a Nutshell
Motivation

- We would like to calculate:

$$\hat{U} = e^{-\beta \hat{H}} \longrightarrow \langle \hat{X} \rangle = \frac{\mathrm{Tr}[\hat{U}\hat{X}]}{\mathrm{Tr}\hat{U}} \qquad (\beta = \frac{1}{T})$$

- Two-body part of $\hat{H}$ causes all the trouble!

SMMC in a Nutshell
Motivation

- We would like to calculate:

$$\hat{U} = e^{-\beta \hat{H}} \longrightarrow \langle \hat{X} \rangle = \frac{\mathrm{Tr}[\hat{U}\hat{X}]}{\mathrm{Tr}\hat{U}} \qquad (\beta = \frac{1}{T})$$

- Two-body part of $\hat{H}$ causes all the trouble! For one-body $\hat{h}$, physics is easy since:

$$e^{-\beta \hat{h}} |\mathrm{SD}\rangle = |\mathrm{SD}'\rangle$$

SMMC in a Nutshell
Motivation

- We would like to calculate:

$$\hat{U} = e^{-\beta\hat{H}} \quad \longrightarrow \quad \langle\hat{X}\rangle = \frac{\mathrm{Tr}[\hat{U}\hat{X}]}{\mathrm{Tr}\hat{U}} \qquad (\beta = \frac{1}{T})$$

- Two-body part of $\hat{H}$ causes all the trouble!
  For one-body $\hat{h}$, physics is easy since:

$$e^{-\beta\hat{h}}|\mathrm{SD}\rangle = |\mathrm{SD}'\rangle$$

$\longrightarrow$ The idea is to *linearize* $\hat{H}$

SMMC in a Nutshell
Hubbard-Stratonovich Transformation

Hamiltonian of the form $\hat{H} = \epsilon\hat{\mathcal{O}} + \frac{1}{2}V\hat{\mathcal{O}}^2$ can be linearized readily:

$$e^{-\beta\hat{H}} = \sqrt{\frac{\beta|V|}{2\pi}} \int_{-\infty}^{\infty} d\sigma e^{-\frac{1}{2}\beta|V|\sigma^2} e^{-\beta\hat{h}}$$

with $\hat{h} = \epsilon\hat{\mathcal{O}} + sV\sigma\hat{\mathcal{O}}$ and

$$s = \begin{cases} 1 & \text{if } V < 0 \\ i & \text{if } V > 0 \end{cases}$$

SMMC in a Nutshell
Hubbard-Stratonovich Transformation

Hamiltonian of the form $\hat{H} = \epsilon\hat{\mathcal{O}} + \frac{1}{2}V\hat{\mathcal{O}}^2$ can be linearized readily:

$$e^{-\beta\hat{H}} = \sqrt{\frac{\beta|V|}{2\pi}} \int_{-\infty}^{\infty} d\sigma e^{-\frac{1}{2}\beta|V|\sigma^2} e^{-\beta\hat{h}}$$

with $\hat{h} = \epsilon\hat{\mathcal{O}} + sV\sigma\hat{\mathcal{O}}$ and

$$s = \begin{cases} 1 & \text{if } V < 0 \\ i & \text{if } V > 0 \end{cases}$$

A typical Hamiltonian has many $\hat{\mathcal{O}}_\alpha$

SMMC in a Nutshell
Hubbard-Stratonovich Transformation

Hamiltonian of the form $\hat{H} = \epsilon\hat{\mathcal{O}} + \frac{1}{2}V\hat{\mathcal{O}}^2$ can be linearized readily:

$$e^{-\beta\hat{H}} = \sqrt{\frac{\beta|V|}{2\pi}}\int_{-\infty}^{\infty} d\sigma e^{-\frac{1}{2}\beta|V|\sigma^2} e^{-\beta\hat{h}}$$

with $\hat{h} = \epsilon\hat{\mathcal{O}} + sV\sigma\hat{\mathcal{O}}$ and

$$s = \begin{cases} 1 & \text{if } V < 0 \\ i & \text{if } V > 0 \end{cases}$$

A typical Hamiltonian has many $\hat{\mathcal{O}}_\alpha$

$\longrightarrow$ Generalize the Gaussian identity

SMMC in a Nutshell
Hubbard-Stratonovich Transformation

Hamiltonian of the form $\hat{H} = \epsilon\hat{\mathcal{O}} + \frac{1}{2}V\hat{\mathcal{O}}^2$ can be linearized readily:

$$e^{-\beta\hat{H}} = \sqrt{\frac{\beta|V|}{2\pi}} \int_{-\infty}^{\infty} d\sigma e^{-\frac{1}{2}\beta|V|\sigma^2} e^{-\beta\hat{h}}$$

with $\hat{h} = \epsilon\hat{\mathcal{O}} + sV\sigma\hat{\mathcal{O}}$ and

$$s = \begin{cases} 1 & \text{if } V < 0 \\ i & \text{if } V > 0 \end{cases}$$

A typical Hamiltonian has many $\hat{\mathcal{O}}_\alpha$

$\longrightarrow$ Generalize the Gaussian identity $\longrightarrow$ *Hubbard-Stratonovich transformation*:

$$Z = \mathrm{Tr}\hat{U} = \mathrm{Tr}e^{-\beta\hat{H}} \longrightarrow \mathrm{Tr}\left[e^{-\Delta\beta\hat{H}}\right]^{N_t} \longrightarrow \int \mathfrak{D}[\sigma]G(\sigma)\mathrm{Tr}\hat{U}_\sigma$$

SMMC in a Nutshell

Hubbard-Stratonovich Transformation

Hamiltonian of the form $\hat{H} = \epsilon\hat{\mathcal{O}} + \frac{1}{2}V\hat{\mathcal{O}}^2$ can be linearized readily:

$$e^{-\beta\hat{H}} = \sqrt{\frac{\beta|V|}{2\pi}} \int_{-\infty}^{\infty} d\sigma e^{-\frac{1}{2}\beta|V|\sigma^2} e^{-\beta\hat{h}}$$

with $\hat{h} = \epsilon\hat{\mathcal{O}} + sV\sigma\hat{\mathcal{O}}$ and

$$s = \begin{cases} 1 & \text{if } V < 0 \\ i & \text{if } V > 0 \end{cases}$$

A typical Hamiltonian has many $\hat{\mathcal{O}}_\alpha$

$\longrightarrow$ Generalize the Gaussian identity $\longrightarrow$ *Hubbard-Stratonovich transformation*:

$$Z = \mathrm{Tr}\hat{U} = \mathrm{Tr}e^{-\beta\hat{H}} \longrightarrow \mathrm{Tr}\left[e^{-\Delta\beta\hat{H}}\right]^{N_t} \longrightarrow \int \mathfrak{D}[\sigma]G(\sigma)\mathrm{Tr}\hat{U}_\sigma$$

where $\hat{U}_\sigma = \prod_{n=1}^{N_t} e^{-\Delta\beta\hat{h}(\sigma)}$

SMMC in a Nutshell
Observables

$$\langle\hat{\Omega}\rangle = \frac{\mathrm{Tr}[\hat{\Omega}e^{-\beta\hat{H}}]}{\mathrm{Tr}e^{-\beta\hat{H}}} = \frac{\int\mathcal{D}[\sigma]G_\sigma\langle\hat{\Omega}\rangle_\sigma\mathrm{Tr}\hat{U}_\sigma}{\int\mathcal{D}[\sigma]G_\sigma\mathrm{Tr}\hat{U}_\sigma} = \frac{\int\mathcal{D}[\sigma]W_\sigma\langle\hat{\Omega}\rangle_\sigma\Phi_\sigma}{\int\mathcal{D}[\sigma]W_\sigma\Phi_\sigma}$$

$\Phi_\sigma = \frac{\mathrm{Tr}\hat{U}_\sigma}{|\mathrm{Tr}\hat{U}_\sigma|}$ Monte-Carlo sign

$W_\sigma = G_\sigma|\mathrm{Tr}\hat{U}_\sigma|$ weight function

$\langle\hat{\Omega}\rangle_\sigma = \frac{\mathrm{Tr}[\hat{\Omega}\hat{U}_\sigma]}{|\mathrm{Tr}\hat{U}_\sigma|}$ observables

SMMC in a Nutshell
Observables

$$\langle\hat{\Omega}\rangle = \frac{\mathrm{Tr}[\hat{\Omega}e^{-\beta\hat{H}}]}{\mathrm{Tr}e^{-\beta\hat{H}}} = \frac{\int\mathcal{D}[\sigma]G_\sigma\langle\hat{\Omega}\rangle_\sigma\mathrm{Tr}\hat{U}_\sigma}{\int\mathcal{D}[\sigma]G_\sigma\mathrm{Tr}\hat{U}_\sigma} = \frac{\int\mathcal{D}[\sigma]W_\sigma\langle\hat{\Omega}\rangle_\sigma\Phi_\sigma}{\int\mathcal{D}[\sigma]W_\sigma\Phi_\sigma}$$

$\Phi_\sigma = \frac{\mathrm{Tr}\hat{U}_\sigma}{|\mathrm{Tr}\hat{U}_\sigma|}$ Monte-Carlo sign

$W_\sigma = G_\sigma|\mathrm{Tr}\hat{U}_\sigma|$ weight function

$\langle\hat{\Omega}\rangle_\sigma = \frac{\mathrm{Tr}[\hat{\Omega}\hat{U}_\sigma]}{|\mathrm{Tr}\hat{U}_\sigma|}$ observables ($\leftarrow$ as in non-interacting problem)

SMMC in a Nutshell
SMMC dissected

Cornerstones of a typical SMMC calculation:

- Decomposition
  Hamiltonian need to be in the quadratic form
  (Pandya transformation)
- Hubbard-Stratonovich transformation
- Calculation of observables
  (Projections if needed)
- Monte-Carlo integration
  (Metropolis algorithm)

SMMC in a Nutshell
Decomposing the Hamiltonian

Consider an individual interaction term $\hat{H} = a_1^\dagger a_2^\dagger a_3 a_4$

Approach 1: *Density decomposition*

$$\hat{H} = \overbrace{a_1^\dagger a_3}\underbrace{a_2^\dagger a_4} - a_1^\dagger a_4 \delta_{23} = -a_1^\dagger a_4 \delta_{23} + \tfrac{1}{2}[a_1^\dagger a_3, a_2^\dagger a_4] + \tfrac{1}{4}(a_1^\dagger a_3 + a_2^\dagger a_4)^2 - \tfrac{1}{4}(a_1^\dagger a_3 - a_2^\dagger a_4)^2$$

Approach 2: *Pairing decomposition*

$$\hat{H} = \overbrace{a_1^\dagger a_2^\dagger}\underbrace{a_4 a_3} = \tfrac{1}{4}(a_1^\dagger a_2^\dagger + a_3 a_4)^2 - \tfrac{1}{4}(a_1^\dagger a_2^\dagger - a_3 a_4)^2 + \tfrac{1}{2}[a_1^\dagger a_2^\dagger, a_3 a_4].$$

Note that the commutator terms are one-body operators.

SMMC in a Nutshell
Shell-model Hamiltonian

$$H = H_1 + H_2 = \sum_{\alpha} \epsilon_\alpha a^\dagger_\alpha a_\alpha + \frac{1}{4} \sum_{\alpha\beta\gamma\delta} V_{\alpha\beta\gamma\delta} a^\dagger_\alpha a^\dagger_\beta a_\delta a_\gamma$$

In the JT-coupled representation, two-body part is written as

$$\begin{aligned} H_2 &= -\frac{1}{4} \sum_{ijkl} \sum_{JT} V^A_{JT}(ij,kl) \left[(2J+1)(2T+1)(1+\delta_{ij})(1+\delta_{kl})\right]^{1/2} \times \\ &\times \left[(a^\dagger_i \otimes a^\dagger_j)^{JT} \otimes (\tilde{a}_k \otimes \tilde{a}_l)^{JT} \right]^{00}_{00} \end{aligned}$$

SMMC in a Nutshell

Shell-model Hamiltonian

$$H = H_1 + H_2 = \sum_{\alpha} \epsilon_\alpha a^\dagger_\alpha a_\alpha + \frac{1}{4}\sum_{\alpha\beta\gamma\delta} V_{\alpha\beta\gamma\delta} a^\dagger_\alpha a^\dagger_\beta a_\delta a_\gamma$$

In the JT-coupled representation, two-body part is written as

$$\begin{aligned} H_2 &= -\frac{1}{4}\sum_{ijkl}\sum_{JT} V^A_{JT}(ij,kl)\left[(2J+1)(2T+1)(1+\delta_{ij})(1+\delta_{kl})\right]^{1/2} \times \\ &\times \left[(a^\dagger_i \otimes a^\dagger_j)^{JT} \otimes (\tilde{a}_k \otimes \tilde{a}_l)^{JT}\right]^{00}_{00} \end{aligned}$$

ϵ_α: single-particle energies

SMMC in a Nutshell
Shell-model Hamiltonian

$$H = H_1 + H_2 = \sum_{\alpha} \epsilon_\alpha a_\alpha^\dagger a_\alpha + \frac{1}{4}\sum_{\alpha\beta\gamma\delta} V_{\alpha\beta\gamma\delta} a_\alpha^\dagger a_\beta^\dagger a_\delta a_\gamma$$

In the JT-coupled representation, two-body part is written as

$$H_2 = -\frac{1}{4}\sum_{ijkl}\sum_{JT} V_{JT}^A(ij,kl)\left[(2J+1)(2T+1)(1+\delta_{ij})(1+\delta_{kl})\right]^{1/2} \times \times \left[(a_i^\dagger \otimes a_j^\dagger)^{JT} \otimes (\tilde{a}_k \otimes \tilde{a}_l)^{JT}\right]_{00}^{00}$$

ϵ_α: single-particle energies
$V_{JT}^A(ij,kl)$: two-body matrix elements

SMMC in a Nutshell
Pandya Transformation

$$\hat{H}_2 \longrightarrow \hat{H}'_2 + \hat{H}'_1 \qquad \text{(Pandya transformation)}$$

$$\hat{H}'_1 = \sum_{ad} \epsilon'_{ad} \hat{\rho}_{0\,0}(a,d)$$

$$\hat{H}'_2 = \frac{1}{2} \sum_{ij} \sum_{K} E_K(i,j) \sum_{M} (-1)^M \hat{\rho}_{KM}(i) \hat{\rho}_{K-M}(j)$$

$\Downarrow$Diagonalize E_K to get $\lambda_{K\alpha}, v_{K\alpha}$

$$= \frac{1}{2} \sum_{K\alpha} \lambda_K(\alpha) \sum_{M \geq 0} \left(\hat{Q}^2_{KM}(\alpha) + \hat{P}^2_{KM}(\alpha) \right)$$

SMMC in a Nutshell

Observables Using Matrix Algebra

$\mathrm{Tr}\hat{U}_\sigma$ and $\langle\hat{O}\rangle_\sigma$ can be evaluated using matrix algebra in the single-particle space. The grand-canonical trace of $\hat{U}_\sigma$ is equivalent to a determinant in the single-particle space:

$$\mathrm{Tr}\hat{U}_\sigma = \det[\mathbf{1} + \mathbf{U}_\sigma]$$

Likewise, observables can be dealt with using matrix algebra in the single-particle space as well:

$$\langle\hat{O}\rangle_\sigma = \frac{\mathrm{Tr}\hat{U}_\sigma\hat{O}}{\mathrm{Tr}\hat{U}_\sigma} = \mathrm{tr}\frac{1}{\mathbf{1} + \mathbf{U}_\sigma}\mathbf{U}_\sigma\mathbf{O}$$

SMMC in a Nutshell

Canonical Ensemble: Particle-number projection

One can extract the canocial many-body traces using the Fourier extraction method:

$$\hat{P}_N = \frac{1}{N_s}\sum_{m=1}^{N_s} e^{-i\phi_m(N-\hat{N})}$$

Particle-number projection

where $\phi_m = \frac{2\pi m}{N_s}$ and $m = 1, \ldots, N_s$

$$\mathrm{Tr}\hat{U}_\sigma \longrightarrow \mathrm{Tr}_N\hat{U}_\sigma = \frac{1}{N_s}\sum_{m=1}^{N_s} e^{-i\phi_m N}\det[\mathbf{1} + e^{i\phi_m}\mathbf{U}_\sigma]$$

Note that $e^{i\phi_m \mathbf{N}}\mathbf{U}_\sigma = e^{i\phi_m}\mathbf{U}_\sigma$ was used above.

SMMC in a Nutshell

Why Monte Carlo Integration

Consider the following integral

$$Z \propto \int \mathrm{d}^3 r_1 \ldots \mathrm{d}^3 r_A e^{-\beta \sum_{i<j} V(r_{ij})}$$

Using a mere 10 pt. mesh for each coordinate, this $3A$-dimensional integral would require 10^{3A} point evaluations. Let $A = 20$, that makes 10^{60} evaluations!

Using a powerful 40 Tflop $(= 4 \times 10^{13}$ processes/sec.) machine, computational time would be:
10^{47} seconds or 10^{30} times the age of the universe!!!

Monte Carlo Integration

$$I = \int \mathrm{d}^d x\, f(x) = \frac{1}{N} \sum_{i=1}^{N} f(x_i)$$

- Uncertainity in the estimate of the integral decreases as $N^{-1/2}$ *independent of the dimension* of the problem!
- In comparison, quadrature errors behave like $\mathcal{O}(N^{-2/d})$

Monte Carlo Integration

$$I = \int \mathrm{d}^d x\, f(x) = \frac{1}{N}\sum_{i=1}^{N} f(x_i)$$

- Uncertainity in the estimate of the integral decreases as $N^{-1/2}$ *independent of the dimension* of the problem!
- In comparison, quadrature errors behave like $\mathcal{O}(N^{-2/d})$

Hence, Monte Carlo wins over quadrature for $d \leq 4$

Monte Carlo Integration

$$I = \int \mathrm{d}^d x\, f(x) = \frac{1}{N} \sum_{i=1}^{N} f(x_i)$$

- Uncertainity in the estimate of the integral decreases as $N^{-1/2}$ *independent of the dimension* of the problem!
- In comparison, quadrature errors behave like $\mathcal{O}(N^{-2/d})$

Hence, Monte Carlo wins over quadrature for $d \leq 4$

As an example, recent SMMC calculations we have performed have 10^5-10^6-dimensional integrals!

SMMC in a Nutshell
Monte Carlo Integration

Monte-Carlo integration (Importance sampling):

$$\frac{\int \mathcal{D}[\sigma] W_\sigma X_\sigma}{\int \mathcal{D}[\sigma] W_\sigma}$$

Sampling according to distribution W is achieved by Metropolis random walk.

SMMC in a Nutshell
Monte Carlo Integration

Monte-Carlo integration (Importance sampling):

$$\frac{\int \mathcal{D}[\sigma] W_\sigma X_\sigma}{\int \mathcal{D}[\sigma] W_\sigma} \longrightarrow \langle X_\sigma \rangle_W = \frac{1}{M} \sum_{k=1}^{M} X_{\sigma(k)}$$

Sampling according to distribution W is achieved by Metropolis random walk.

SMMC in a Nutshell
Monte Carlo Integration

Monte-Carlo integration (Importance sampling):

$$\frac{\int \mathcal{D}[\sigma] W_\sigma X_\sigma}{\int \mathcal{D}[\sigma] W_\sigma} \longrightarrow \langle X_\sigma \rangle_W = \frac{1}{M} \sum_{k=1}^{M} X_{\sigma(k)}$$

Sampling according to distribution W is achieved by Metropolis random walk.

Thus we obtain $\langle \hat{\Omega} \rangle = \frac{\int \mathcal{D}[\sigma] W_\sigma \langle \hat{\Omega} \rangle_\sigma \Phi_\sigma}{\int \mathcal{D}[\sigma] W_\sigma \Phi_\sigma} = \frac{\langle \langle \hat{\Omega}_\sigma \rangle \Phi_\sigma \rangle_W}{\langle \Phi_\sigma \rangle_W}$.

SMMC in a Nutshell

Generating the Samples: Metropolis Algorithm

Field configurations $\sigma_1, \sigma_2, \ldots$ that are randomly distributed according to a probability distribution W, can be generated by repeating the following procedure:

SMMC in a Nutshell
Generating the Samples: Metropolis Algorithm

Field configurations $\sigma_1, \sigma_2, \ldots$ that are randomly distributed according to a probability distribution W, can be generated by repeating the following procedure:

1. Start with some initial configuration σ_i

SMMC in a Nutshell

Generating the Samples: Metropolis Algorithm

Field configurations $\sigma_1, \sigma_2, \ldots$ that are randomly distributed according to a probability distribution W, can be generated by repeating the following procedure:

1. Start with some initial configuration σ_i
2. Move to a trial configuration σ_t

SMMC in a Nutshell

Generating the Samples: Metropolis Algorithm

Field configurations $\sigma_1, \sigma_2, \ldots$ that are randomly distributed according to a probability distribution W, can be generated by repeating the following procedure:

1. Start with some initial configuration σ_i
2. Move to a trial configuration σ_t
3. Calculate the ratio $r = \frac{W(\sigma_t)}{W(\sigma_i)}$

SMMC in a Nutshell

Generating the Samples: Metropolis Algorithm

Field configurations $\sigma_1, \sigma_2, \ldots$ that are randomly distributed according to a probability distribution W, can be generated by repeating the following procedure:

1. Start with some initial configuration σ_i
2. Move to a trial configuration σ_t
3. Calculate the ratio $r = \frac{W(\sigma_t)}{W(\sigma_i)}$
4. If $r > 1$ then *accept the trial move*, i.e., $\sigma_{i+1} = \sigma_t$
   Otherwise
   accept the trial move with probability r.

SMMC in a Nutshell

Generating the Samples: Metropolis Algorithm

Field configurations $\sigma_1, \sigma_2, \ldots$ that are randomly distributed according to a probability distribution W, can be generated by repeating the following procedure:

1. Start with some initial configuration σ_i
2. Move to a trial configuration σ_t
3. Calculate the ratio $r = \frac{W(\sigma_t)}{W(\sigma_i)}$
4. If $r > 1$ then *accept the trial move*, i.e., $\sigma_{i+1} = \sigma_t$
   Otherwise
   accept the trial move with probability r.
5. Go to step 1.

SMMC in a Nutshell
In Summary . . .

- Eigenvalue problem $\longrightarrow$ Quadrature (combinatorial scaling $\longrightarrow N_s^2 N_t$)

SMMC in a Nutshell

In Summary . . .

- Eigenvalue problem $\longrightarrow$ Quadrature
  (combinatorial scaling $\longrightarrow$ $N_s^2 N_t$)
- Many-body nature $\longrightarrow$ one-body nature in fluctuating fields

SMMC in a Nutshell

In Summary . . .

- Eigenvalue problem $\longrightarrow$ Quadrature
  (combinatorial scaling $\longrightarrow N_s^2 N_t$)
- Many-body nature $\longrightarrow$ one-body nature in fluctuating fields
- Operators $\longrightarrow$ matrices of dimension $N_s \times N_s$
  (*e.g.*, $\hat{U}_\sigma \longrightarrow \mathbf{U}_\sigma$)

SMMC in a Nutshell
In Summary . . .

- Eigenvalue problem $\longrightarrow$ Quadrature (combinatorial scaling $\longrightarrow N_s^2 N_t$)
- Many-body nature $\longrightarrow$ one-body nature in fluctuating fields
- Operators $\longrightarrow$ matrices of dimension $N_s \times N_s$ (*e.g.*, $\hat{U}_\sigma \longrightarrow \mathbf{U}_\sigma$)
- Exact upto controllable discretization and sampling errors

Sign Problem

Often the sign $\Phi_\sigma = \frac{\mathrm{Tr}U_\sigma}{|\mathrm{Tr}U_\sigma|}$ is not positive for some of the samples σ! When $\langle \Phi_\sigma \rangle_W \to 0$, variance in the MC integral

$$\langle \hat{\Omega} \rangle = \frac{\langle \langle \hat{\Omega}_\sigma \rangle \Phi_\sigma \rangle_W}{\langle \Phi_\sigma \rangle_W}$$

rapidly becomes too large and the method fails!

Most effective nuclear interactions suffer from the sign problem, and the problem gets worse at lower temperatures.

Sign problem and Time-reversal Symmetry

It can be shown that if the linearized Hamiltonian $\hat{h}_\sigma$ is time-reversally symmetric, then eigenvalues of $\mathbf{U}_\sigma$ come in complex-conjugate pairs, implying

$$\mathrm{Tr}\hat{U} = \det\left[\mathbf{1} + \mathbf{U}\right] = \prod_{\lambda}^{N_s/2} (1+\epsilon_\lambda)(1+\epsilon_\lambda^*) > 0.$$

Grand-canonical case

as a results $\Phi_\sigma = 1$ is guaranteed.

Sign problem and Time-reversal Symmetry

It can be shown that if the linearized Hamiltonian $\hat{h}_\sigma$ is time-reversally symmetric, then eigenvalues of $\mathbf{U}_\sigma$ come in complex-conjugate pairs, implying

$$\mathrm{Tr}\hat{U} = \det\left[\mathbf{1} + \mathbf{U}\right] = \prod_{\lambda}^{N_s/2} (1+\epsilon_\lambda)(1+\epsilon_\lambda^*) > 0.$$

Grand-canonical case

as a results $\Phi_\sigma = 1$ is guaranteed.

What is the condition for $\hat{\bar{h}}_\sigma = \hat{h}_\sigma$ then?

Sign Problem and the Time-reversal Symmetry

$\hat{H}$ always obeys the time-reversal symmetry. Explicitly

$$\hat{H} = \sum_i \epsilon_i a_i^\dagger a_i + \frac{1}{2} \sum_\alpha \lambda_\alpha \{\hat{\rho}_\alpha, \hat{\bar{\rho}}_\alpha\}$$

where λ_α are real and $\hat{\rho}_\alpha = \sum_{ij} C_{ij}^\alpha \hat{\rho}_{ij}$. The linearized Hamiltonian

$$\hat{h}_\sigma(\tau_n) = \sum_i \epsilon_\alpha a_i^\dagger a_i + \sum_\alpha (s_\alpha \lambda_\alpha \sigma_{\alpha n} \hat{\rho}_\alpha + s_\alpha \lambda_\alpha \sigma_{\alpha n}^* \hat{\bar{\rho}}_\alpha).$$

Sign Problem and the Time-reversal Symmetry

$\hat{H}$ always obeys the time-reversal symmetry. Explicitly

$$\hat{H} = \sum_i \epsilon_i a_i^\dagger a_i + \frac{1}{2} \sum_\alpha \lambda_\alpha \{\hat{\rho}_\alpha, \hat{\bar{\rho}}_\alpha\}$$

where λ_α are real and $\hat{\rho}_\alpha = \sum_{ij} C_{ij}^\alpha \hat{\rho}_{ij}$. The linearized Hamiltonian

$$\hat{h}_\sigma(\tau_n) = \sum_i \epsilon_\alpha a_i^\dagger a_i + \sum_\alpha (s_\alpha \lambda_\alpha \sigma_{\alpha n} \hat{\rho}_\alpha + s_\alpha \lambda_\alpha \sigma_{\alpha n}^* \hat{\bar{\rho}}_\alpha).$$

is time-reversal symmetric

if $\lambda_\alpha < 0$ then $\hat{\bar{h}}_\sigma = \hat{h}_\sigma$

A Practical Solution to the Sign Problem

An extrapolation method

A given Hamiltonian is decomposed into *good* and *bad* parts:

$$\hat{H}_G = \sum_i \epsilon_i a_i^\dagger a_i + \frac{1}{2} \sum_{\lambda_\alpha < 0} \lambda_\alpha \{\hat{\rho}_\alpha, \bar{\hat{\rho}}_\alpha\},$$

$$\hat{H}_B = \frac{1}{2} \sum_{\lambda_\alpha > 0} \lambda_\alpha \{\hat{\rho}_\alpha, \bar{\hat{\rho}}_\alpha\}$$

Construct a new, "*sign-free*" family of Hamiltonians

$H_g = f(g) H_G + g H_B$ with $f(g < 0) > 0$ and $\hat{H}_{g=1} = \hat{H}$

Note that $\Phi_\sigma = 1$ for $g \leq 0$ by construction.

Y. Alhassid *et. al*, Phys. Rev. Lett. **72** 613, 1994.

Example to the Extrapolation Method

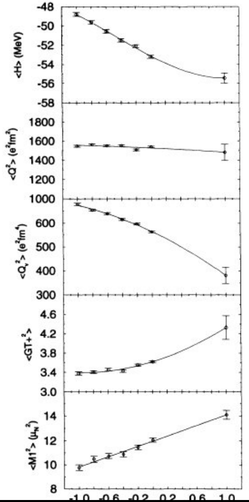

Calculate

$$\langle \hat{O} \rangle_g = \frac{\mathrm{Tr}[\hat{O} e^{-\beta \hat{H}_g}]}{\mathrm{Tr}[e^{-\beta \hat{H}_g}]}$$

then use a polynomial extrapolation to get the physical value $\langle \hat{O} \rangle_{g=1}$.

In the case of energy, variational principle imposes the extra condition:

$$\left. \frac{d\langle H \rangle_g}{dg} \right|_{g=1} = 0$$

Effective Interactions without the Sign Problem

effective nuclear int. $\approx$ collective part $+$ non-collective part

Effective Interactions without the Sign Problem

$$\text{effective nuclear int.} \approx \underset{\substack{\text{gives } \textit{good} \text{ sign} \\ \text{important for level densities}}}{\underset{\downarrow}{\text{collective part}}} + \underset{\substack{\text{gives } \textit{bad} \text{ sign} \\ \text{not so important for level density}}}{\underset{\downarrow}{\text{non-collective part}}}$$

Effective Interactions without the Sign Problem

effective nuclear int. $\approx$ collective part $+$ non-collective part

collective part $\downarrow$ gives *good* sign, important for level densities

non-collective part $\downarrow$ gives *bad* sign, not so important for level density

Example: *Pairing+Quadrupole Interaction*

$$\hat{H} = \sum_{\alpha} \epsilon_\alpha a^\dagger_\alpha a_\alpha - \chi \sum_{\mu} (-1)^\mu \hat{Q}_{2\mu} \hat{Q}_{2-\mu} - \frac{G}{4} \sum_{\alpha,\alpha',t_z} P^\dagger_{JT=01,t_z}(\alpha) P_{JT=01,t_z}(\alpha')$$

where $\hat{Q}_{2\mu}$ is the mass quadrupole operator: $\hat{Q}_{2\mu} = \frac{1}{\sqrt{5}} \sum_{ab} \langle j_a || \frac{dV_{WS}}{dr} Y_2 || j_b \rangle [a^\dagger_{j_a} \otimes \tilde{a}_{j_b}]^{2\mu}$

and $P^\dagger_{JT=01,t_z}(\alpha)$ is the seniority pairing operator: $P^\dagger_{JT=01,t_z}(\alpha) = (-1)^l \left[a^\dagger_{\alpha,t_z} \otimes a_{\alpha,t_z} \right]^{JM=00,T=1}$

Stabilizing the SMMC Against the Sign Problem

Shifted Contour Method

Standard SMMC:

$$\hat{H} = \sum_\alpha \epsilon_\alpha \hat{O}_\alpha + \frac{1}{2}\sum_\alpha \lambda_\alpha \hat{O}_\alpha^2$$

$$e^{-\frac{1}{2}\Delta\beta\lambda\hat{O}^2} = \sqrt{\frac{\Delta\beta|\lambda|}{2\pi}} \int d\sigma \; e^{-\frac{1}{2}\Delta\beta|\lambda|\sigma^2 - \Delta\beta s\sigma\lambda\hat{O}}$$

Shifted-contour SMMC:

$$\hat{H} = \sum_\alpha (\epsilon_\alpha - W_\alpha)\hat{O}_\alpha + \frac{1}{2}\sum_\alpha \lambda_\alpha (\hat{O}_\alpha - \tilde{O}_\alpha)^2$$

$$e^{-\frac{1}{2}\Delta\beta\lambda\hat{O}^2} = \sqrt{\frac{\Delta\beta|\lambda|}{2\pi}} \int d\sigma \; e^{-\frac{1}{2}\Delta\beta|\lambda|(\sigma - s\tilde{O})^2 - \Delta\beta s(\sigma - s\tilde{O})\lambda\hat{O}}$$

R. Baer, M. Head-Gordon and D. Neuhauser, J. Chem. Phys. **109** 6219, 1998

Stabilizing the SMMC Against the Sign Problem
Shifted Contour Method

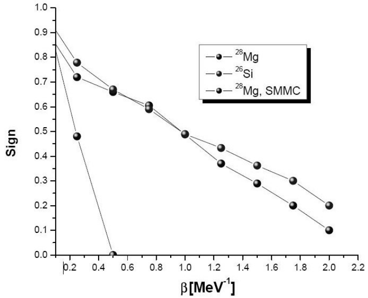

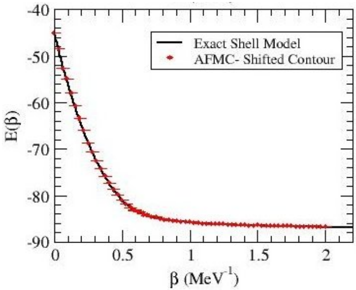

Sign problem delayed. Courtesy of G. Stoitcheva

To Be Continued...

So far we have seen a mostly abstract background of the technique. It is time we continue with some applications ...

Examples from Applications of the SMMC Method

Thermal Properties of Nuclei

Thermal Properties of Nuclei

Some Questions

In finite many-body systems, surface effects and associated quantum fluctuations make the concept of distinct phases a fuzzy concept.

- Can one find signatures of phase transitions? Paired to unpaired, deformed to spherical
- How are pairing correlations and deformation affected by temperature?
  In particular, how do the quadrupole shape deformations (which favors low-density of single-particle states around Fermi level) and pairing collectivity (which tries to restore spherical symmetry) compete?

Pairing Correlations

A measure for BCS-like $J = 0$, $T = 1$ pairing correlations in the ground state is $\langle \Delta_p^\dagger \Delta_p \rangle$ (for protons) where

$$\Delta_p^\dagger = \sum_{jm>0} p_{jm}^\dagger p_{j\bar{m}}^\dagger$$

For genuine correlations one must consider the excess over the uncorrelated Fermi gas value

$$\langle \Delta^\dagger \Delta \rangle = \sum_j \frac{n_j}{2(2j+1)}$$

where $n_j = \sum_m a_{jm}^\dagger a_{jm}$ are the occupation numbers.

Pairing Correlations

$$A^{\dagger}_{JM}(j_a j_b) = \frac{1}{\sqrt{1+\delta_{ab}}}[a^{\dagger}_{j_a} \otimes a^{\dagger}_{j_b}]^{JM}$$

pp- or nn-pairing

pn-pairing

$$A^{\dagger}_{JM}(j_a j_b) = \frac{1}{\sqrt{2(1+\delta_{ab})}}\left\{[a^{\dagger}_{\pi j_a} \otimes a^{\dagger}_{\nu j_b}]^{JM} \pm [a^{\dagger}_{\nu j_a} \otimes a^{\dagger}_{\pi j_b}]^{JM}\right\}$$

$$\left(\begin{array}{l} +\text{ for T=0} \\ -\text{ for T=1} \end{array}\right)$$

$$M^{J}_{\alpha,\alpha'} = \sum_{M} \langle A^{\dagger}_{JM}(j_a j_b) A_{JM}(j_c j_d)\rangle$$

An often-used, convenient measure of pairing correlations is

$$P(J) = \sum_{\alpha \geq \alpha'} M^{J}_{\alpha,\alpha'}$$

Genuine pair correlations are obtained as

$$P_{corr}(J) = P(J) - P_{MF}(J)$$

Thermal Properties of $N = 40$ Isotones

Nuclei around $A \sim 72$ are capable of developing large deformations and strong pairing correlations in their ground states.
Consider the following $N = 40$ nuclei:

- ^{68}Ni spherical, weak pairing corr.
- ^{70}Zn spherical, strong pairing corr.
- ^{72}Ge shape coexistence
- ^{80}Zr well-deformed, weak pairing corr.

Thermal Properties of $N = 40$ Isotones

Specific Heat

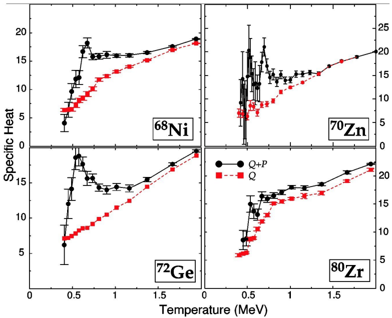

K. Langanke, D.J. Dean and W. Nazarewicz, Nucl. Phys. **A757** 360, 2005.

Thermal Properties of $N = 40$ Isotones

Specific Heat

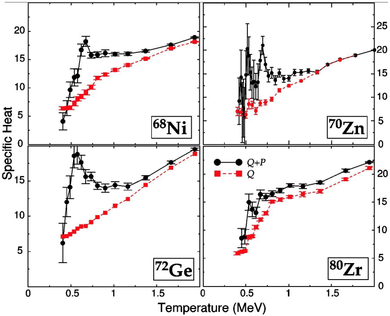

- No peaks observed when P term is off

K. Langanke, D.J. Dean and W. Nazarewicz, Nucl. Phys. **A757** 360, 2005.

Thermal Properties of $N = 40$ Isotones

Specific Heat

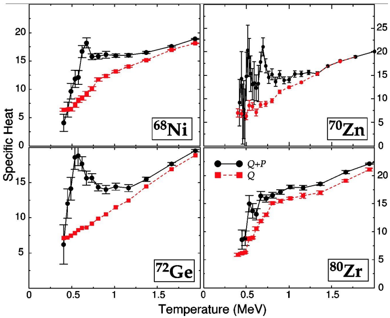

- No peaks observed when P term is off
- ^{80}Zr has a shoulder signalling deformation change

K. Langanke, D.J. Dean and W. Nazarewicz, Nucl. Phys. **A757** 360, 2005.

Thermal Properties of $N = 40$ Isotones

Specific Heat

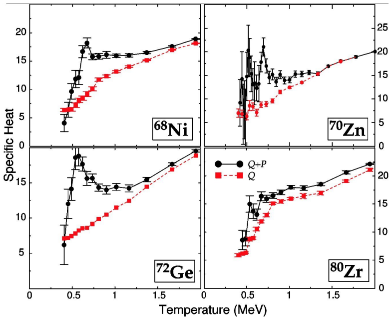

- No peaks observed when P term is off
- ^{80}Zr has a shoulder signalling deformation change
- Turning P on, enhances pair correlations ^{72}Ge and ^{70}Zn develop peaks

K. Langanke, D.J. Dean and W. Nazarewicz, Nucl. Phys. **A757** 360, 2005.

Thermal Properties of $N = 40$ Isotones

Specific Heat

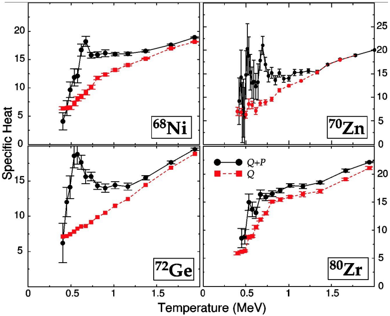

- No peaks observed when P term is off
- ^{80}Zr has a shoulder signalling deformation change
- Turning P on, enhances pair correlations ^{72}Ge and ^{70}Zn develop peaks
- Distinction of *static* vs. *dynamic* pairing correlations

K. Langanke, D.J. Dean and W. Nazarewicz, Nucl. Phys. **A757** 360, 2005.

Thermal Properties of $N = 40$ Isotones

Specific Heat

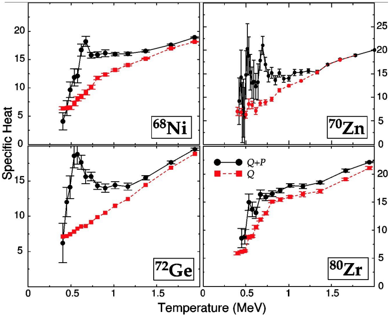

- No peaks observed when P term is off
- ^{80}Zr has a shoulder signalling deformation change
- Turning P on, enhances pair correlations ^{72}Ge and ^{70}Zn develop peaks
- Distinction of *static* vs. *dynamic* pairing correlations
- All pairing correlations are destroyed at sufficiently high T

K. Langanke, D.J. Dean and W. Nazarewicz, Nucl. Phys. **A757** 360, 2005.

Thermal Properties of $N = 40$ Isotones

$B(E2)$ Strength

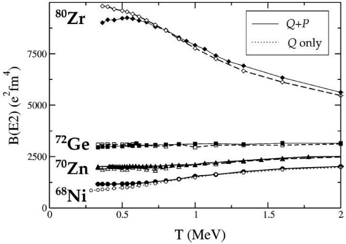

$B(E2)$ strenght as a measure of quadrupole deformation

$\langle Q^2 \rangle$ with $Q_{2\mu} = Q_{2\mu}^{(p)} + Q_{2\mu}^{(n)}$ where $Q_{2\mu}^{(p/n)} = e_{p/n} \sum_{i_{p/n}} r_i^2 Y_{2\mu}(\theta_i, \phi_i)$

K. Langanke, D.J. Dean and W. Nazarewicz, Nucl. Phys. **A757** 360, 2005.

Thermal Properties of $N = 40$ Isotones

$B(E2)$ Strength

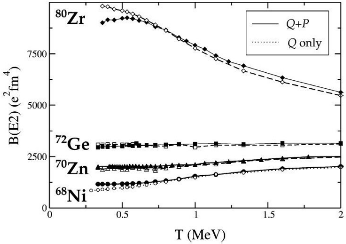

- ^{80}Zr goes through a smooth shape transition

$B(E2)$ strenght as a measure of quadrupole deformation

$\langle Q^2 \rangle$ with $Q_{2\mu} = Q_{2\mu}^{(p)} + Q_{2\mu}^{(n)}$ where $Q_{2\mu}^{(p/n)} = e_{p/n} \sum_{i_{p/n}} r_i^2 Y_{2\mu}(\theta_i, \phi_i)$

K. Langanke, D.J. Dean and W. Nazarewicz, Nucl. Phys. **A757** 360, 2005.

Thermal Properties of $N = 40$ Isotones
$B(E2)$ Strength

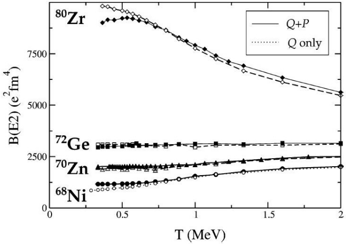

- ^{80}Zr goes through a smooth shape transition
- Effect of turning on P turns out to be negligible. Only in ^{80}Zr at low T pairing restores symmetry though weakly.

$B(E2)$ strenght as a measure of quadrupole deformation

$\langle Q^2 \rangle$ with $Q_{2\mu} = Q_{2\mu}^{(p)} + Q_{2\mu}^{(n)}$ where $Q_{2\mu}^{(p/n)} = e_{p/n} \sum_{i_{p/n}} r_i^2 Y_{2\mu}(\theta_i, \phi_i)$

K. Langanke, D.J. Dean and W. Nazarewicz, Nucl. Phys. **A757** 360, 2005.

Thermal Properties of $N = 40$ Isotones

$B(E2)$ Strength

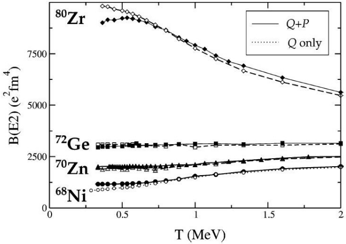

- ^{80}Zr goes through a smooth shape transition
- Effect of turning on P turns out to be negligible. Only in ^{80}Zr at low T pairing restores symmetry though weakly.
- Effect of turning on P in ^{68}Ni is counterintuitive. Pairing scatters nucleons from fp to gds, increased $g_{9/2}$ occupation along with strong $g_{9/2} - f_{5/2}$ coupling enhances deformation.

$B(E2)$ strenght as a measure of quadrupole deformation

$\langle Q^2 \rangle$ with $Q_{2\mu} = Q_{2\mu}^{(p)} + Q_{2\mu}^{(n)}$ where $Q_{2\mu}^{(p/n)} = e_{p/n} \sum_{i_{p/n}} r_i^2 Y_{2\mu}(\theta_i, \phi_i)$

K. Langanke, D.J. Dean and W. Nazarewicz, Nucl. Phys. **A757** 360, 2005.

Thermal Properties of $N = 40$ Isotones

Pairing strength

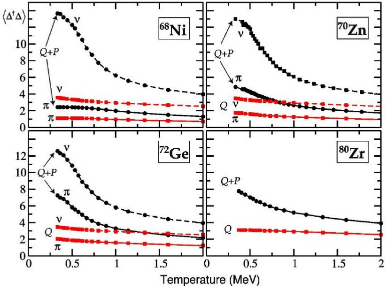

K. Langanke, D.J. Dean and W. Nazarewicz, Nucl. Phys. **A757** 360, 2005.

Thermal Properties of $N = 40$ Isotones

Pairing strength

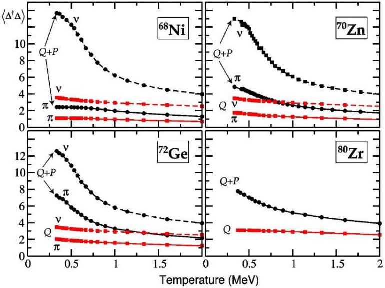

- Pairing correlations enhanced in all cases with turning on P.

K. Langanke, D.J. Dean and W. Nazarewicz, Nucl. Phys. **A757** 360, 2005.

Thermal Properties of $N = 40$ Isotones

Pairing strength

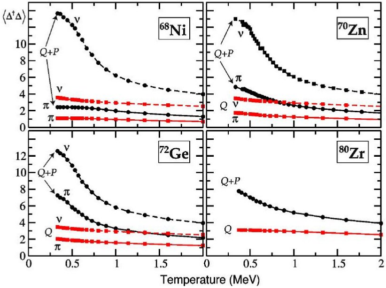

- Pairing correlations enhanced in all cases with turning on P.
- ^{68}Ni has very weak proton pairing, explaining the corresponding peak in specific heat.

K. Langanke, D.J. Dean and W. Nazarewicz, Nucl. Phys. **A757** 360, 2005.

Thermal Properties of $N = 40$ Isotones

Pairing strength

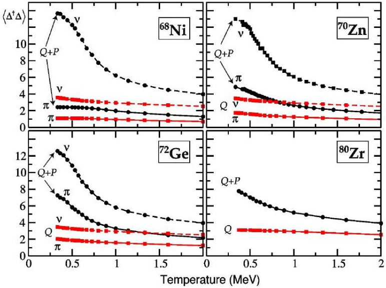

- Pairing correlations enhanced in all cases with turning on P.
- ^{68}Ni has very weak proton pairing, explaining the corresponding peak in specific heat.
- Behaviour of decreasing pairing strength in ^{70}Zn and ^{72}Ge explains the corresponding peak structures in specific heat plot.

K. Langanke, D.J. Dean and W. Nazarewicz, Nucl. Phys. **A757** 360, 2005.

Thermal Properties of $N = 40$ Isotones

Pairing strength

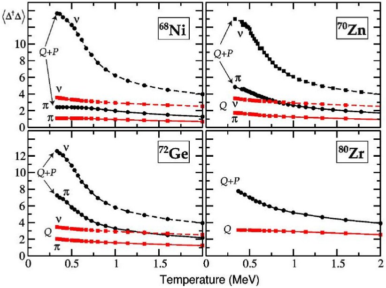

- Pairing correlations enhanced in all cases with turning on P.
- ^{68}Ni has very weak proton pairing, explaining the corresponding peak in specific heat.
- Behaviour of decreasing pairing strength in ^{70}Zn and ^{72}Ge explains the corresponding peak structures in specific heat plot.
- Rather gentle diassociation of pairs in ^{80}Zr points to dynamic pairing effect.

K. Langanke, D.J. Dean and W. Nazarewicz, Nucl. Phys. **A757** 360, 2005.

Thermal Properties of $N = 40$ Isotones

Nuclear Shapes

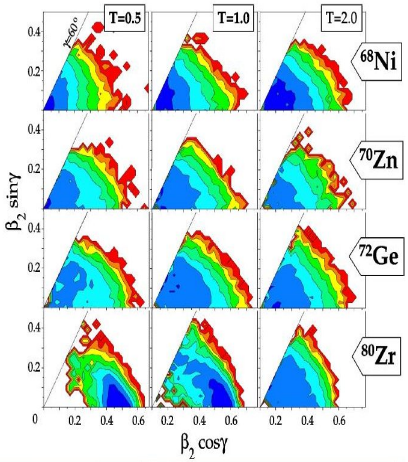

Thermal Properties of $N = 40$ Isotones

Shape and pairing changes manisfests themselves in different ways:

Thermal Properties of $N = 40$ Isotones

Shape and pairing changes manisfests themselves in different ways:

- Superfluid (static pairing)-to-normal transition is associated with a peak in the specific heat around $T \approx 0.6 - 0.7$ MeV

Thermal Properties of $N = 40$ Isotones

Shape and pairing changes manisfests themselves in different ways:

- Superfluid (static pairing)-to-normal transition is associated with a peak in the specific heat around $T \approx 0.6 - 0.7$ MeV
- Deformed-to-spherical transition is fairly gradual. Changes in dynamic pairing does not manifest a peak in the specific heat. Hence the notion of a phase transition does not apply.

Pairing Correlations

^{72}Ge $\rightarrow$ (12, 20)	^{80}Zr $\rightarrow$ (40, 40)
^{71}Ga $\rightarrow$ (11, 20)	^{75}Ge $\rightarrow$ (12, 23)
^{70}Ga $\rightarrow$ (11, 19)	^{76}As $\rightarrow$ (13, 23)

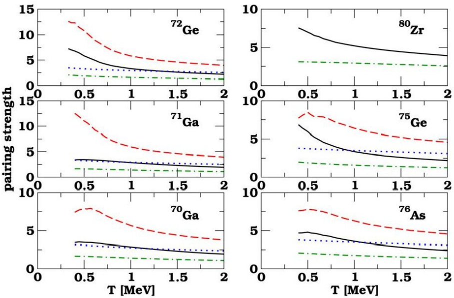

Pairing Correlations

^{72}Ge $\rightarrow$ (12, 20)	^{80}Zr $\rightarrow$ (40, 40)
^{71}Ga $\rightarrow$ (11, 20)	^{75}Ge $\rightarrow$ (12, 23)
^{70}Ga $\rightarrow$ (11, 19)	^{76}As $\rightarrow$ (13, 23)

- Accidental pairing in $Q.Q$-only case

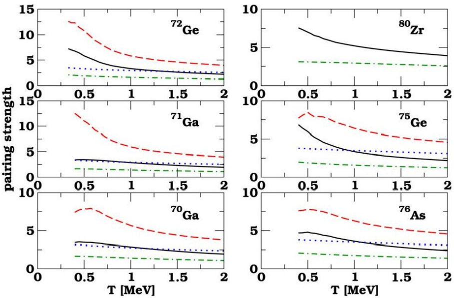

Pairing Correlations

^{72}Ge $\longrightarrow$ (12, 20)
^{71}Ga $\longrightarrow$ (11, 20)
^{70}Ga $\longrightarrow$ (11, 19)
^{80}Zr $\longrightarrow$ (40, 40)
^{75}Ge $\longrightarrow$ (12, 23)
^{76}As $\longrightarrow$ (13, 23)

- Accidental pairing in $Q.Q$-only case
- Enhanced pair correlations with $P^\dagger P$ "on"

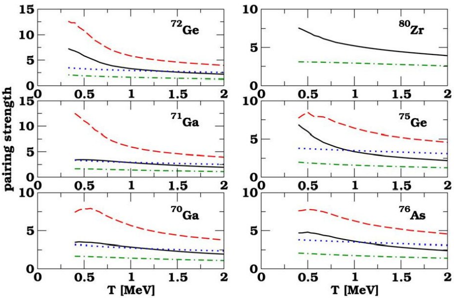

Pairing Correlations

^{72}Ge $\longrightarrow$ (12, 20) ^{80}Zr $\longrightarrow$ (40, 40)
^{71}Ga $\longrightarrow$ (11, 20) ^{75}Ge $\longrightarrow$ (12, 23)
^{70}Ga $\longrightarrow$ (11, 19) ^{76}As $\longrightarrow$ (13, 23)

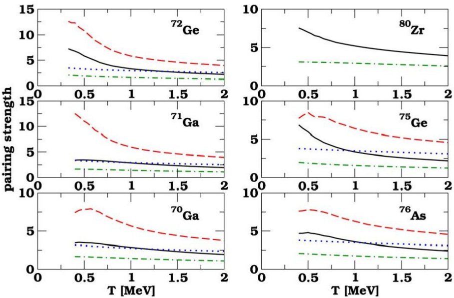

- Accidental pairing in $Q.Q$-only case
- Enhanced pair correlations with $P^\dagger P$ "on"
- Larger pair correlations for even number of nucleons

Pairing Correlations

^{72}Ge $\rightarrow$ (12, 20)
^{71}Ga $\rightarrow$ (11, 20)
^{70}Ga $\rightarrow$ (11, 19)
^{80}Zr $\rightarrow$ (40, 40)
^{75}Ge $\rightarrow$ (12, 23)
^{76}As $\rightarrow$ (13, 23)

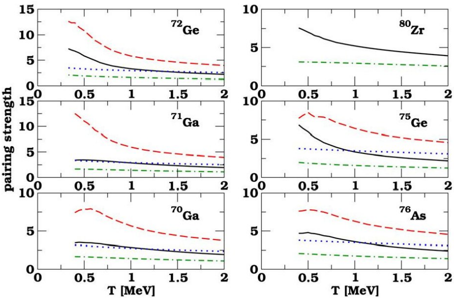

- Accidental pairing in $Q.Q$-only case
- Enhanced pair correlations with $P^\dagger P$ "on"
- Larger pair correlations for even number of nucleons
- Compare ^{72}Ge to ^{71}Ga and ^{72}Ge to ^{75}Ge
  Decoupled fluids

Pairing Correlations

^{72}Ge $\longrightarrow$ (12, 20) ^{80}Zr $\longrightarrow$ (40, 40)
^{71}Ga $\longrightarrow$ (11, 20) ^{75}Ge $\longrightarrow$ (12, 23)
^{70}Ga $\longrightarrow$ (11, 19) ^{76}As $\longrightarrow$ (13, 23)

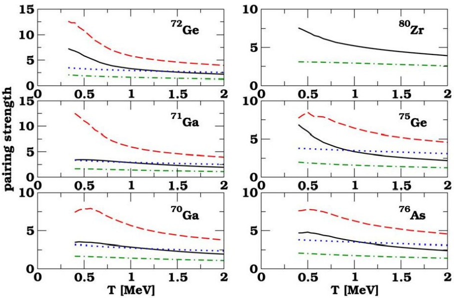

- Accidental pairing in $Q.Q$-only case
- Enhanced pair correlations with $P^\dagger P$ "on"
- Larger pair correlations for even number of nucleons
- Compare ^{72}Ge to ^{71}Ga and ^{72}Ge to ^{75}Ge
  Decoupled fluids
- ^{80}Zr being $N = Z \longrightarrow$ relative reduction

Pairing Correlations

^{72}Ge $\longrightarrow$ (12, 20) ^{80}Zr $\longrightarrow$ (40, 40)
^{71}Ga $\longrightarrow$ (11, 20) ^{75}Ge $\longrightarrow$ (12, 23)
^{70}Ga $\longrightarrow$ (11, 19) ^{76}As $\longrightarrow$ (13, 23)

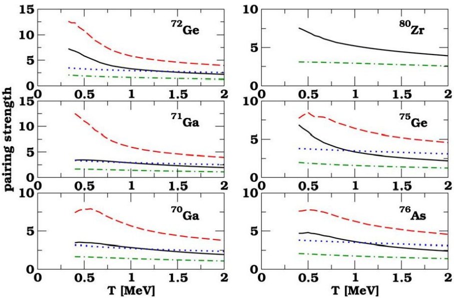

- Accidental pairing in $Q.Q$-only case
- Enhanced pair correlations with $P^\dagger P$ "on"
- Larger pair correlations for even number of nucleons
- Compare ^{72}Ge to ^{71}Ga and ^{72}Ge to ^{75}Ge
  Decoupled fluids
- ^{80}Zr being $N = Z \longrightarrow$ relative reduction
- Faster breaking of genuine pairing correlations with increasing T

Pairing Correlations

^{72}Ge $\longrightarrow$ (12, 20) ^{80}Zr $\longrightarrow$ (40, 40)
^{71}Ga $\longrightarrow$ (11, 20) ^{75}Ge $\longrightarrow$ (12, 23)
^{70}Ga $\longrightarrow$ (11, 19) ^{76}As $\longrightarrow$ (13, 23)

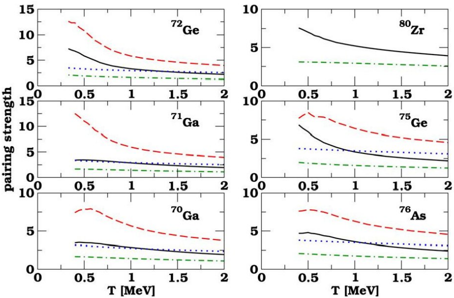

- Accidental pairing in $Q.Q$-only case
- Enhanced pair correlations with $P^\dagger P$ "on"
- Larger pair correlations for even number of nucleons
- Compare ^{72}Ge to ^{71}Ga and ^{72}Ge to ^{75}Ge
  Decoupled fluids
- ^{80}Zr being $N = Z \longrightarrow$ relative reduction
- Faster breaking of genuine pairing correlations with increasing T
- Low T behaviour for odd-number of nucleon case: blocking

Pairing Correlations
Specific Heat

^{72}Ge $\longrightarrow$ (12, 20)
^{71}Ga $\longrightarrow$ (11, 20)
^{70}Ga $\longrightarrow$ (11, 19)

^{80}Zr $\longrightarrow$ (40, 40)
^{75}Ge $\longrightarrow$ (12, 23)
^{76}As $\longrightarrow$ (13, 23)

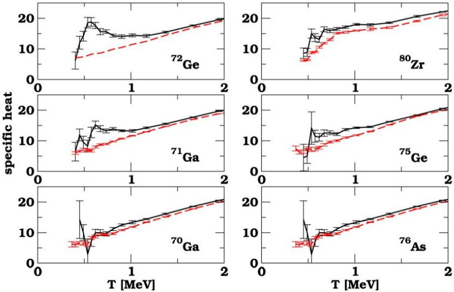

Pairing Correlations
Specific Heat

^{72}Ge $\rightarrow$ (12, 20) ^{80}Zr $\rightarrow$ (40, 40)
^{71}Ga $\rightarrow$ (11, 20) ^{75}Ge $\rightarrow$ (12, 23)
^{70}Ga $\rightarrow$ (11, 19) ^{76}As $\rightarrow$ (13, 23)

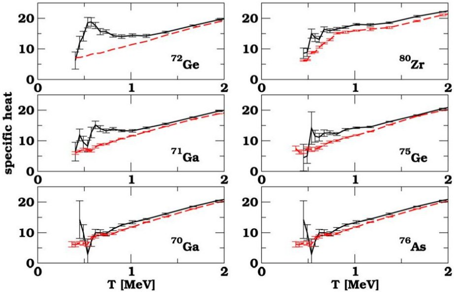

- Pronounced peak for even number of nucleons $\longrightarrow$ paired-to-unpaired transition

Pairing Correlations
Specific Heat

^{72}Ge $\rightarrow$ (12, 20)	^{80}Zr $\rightarrow$ (40, 40)
^{71}Ga $\rightarrow$ (11, 20)	^{75}Ge $\rightarrow$ (12, 23)
^{70}Ga $\rightarrow$ (11, 19)	^{76}As $\rightarrow$ (13, 23)

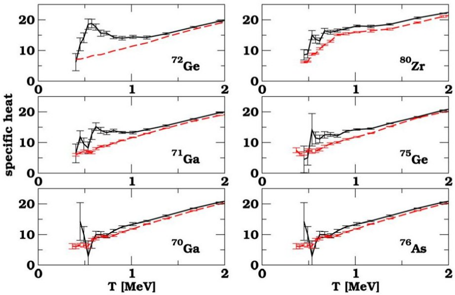

- Pronounced peak for even number of nucleons $\longrightarrow$ paired-to-unpaired transition
- Strongly-deformed ^{80}Zr has less pronounced peak

Pairing Correlations
Specific Heat

^{72}Ge $\longrightarrow$ (12, 20)	^{80}Zr $\longrightarrow$ (40, 40)
^{71}Ga $\longrightarrow$ (11, 20)	^{75}Ge $\longrightarrow$ (12, 23)
^{70}Ga $\longrightarrow$ (11, 19)	^{76}As $\longrightarrow$ (13, 23)

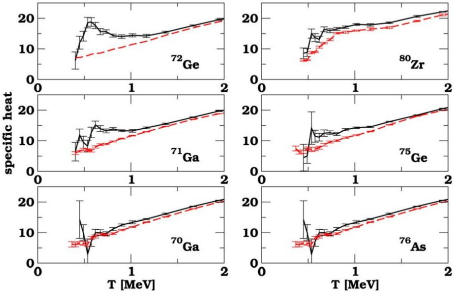

- Pronounced peak for even number of nucleons $\longrightarrow$ paired-to-unpaired transition
- Strongly-deformed ^{80}Zr has less pronounced peak
- Compare ^{72}Ge to ^{71}Ga (even-even vs odd-even) *less pronounced peak in odd-even case*

Pairing Correlations
Specific Heat

^{72}Ge $\rightarrow$ (12, 20)	^{80}Zr $\rightarrow$ (40, 40)
^{71}Ga $\rightarrow$ (11, 20)	^{75}Ge $\rightarrow$ (12, 23)
^{70}Ga $\rightarrow$ (11, 19)	^{76}As $\rightarrow$ (13, 23)

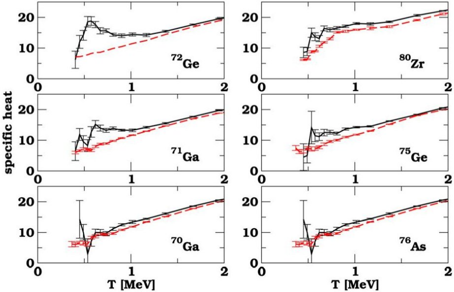

- Pronounced peak for even number of nucleons $\longrightarrow$ paired-to-unpaired transition
- Strongly-deformed ^{80}Zr has less pronounced peak
- Compare ^{72}Ge to ^{71}Ga (even-even vs odd-even) *less pronounced peak in odd-even case*
- Double-peak structure in ^{71}Ga *not so obvious, needs to be understood*

Calculation of Nuclear level Densities

Nuclear Level Density

Nuclear level density is the number of nuclear levels per excitation energy at a given excitation energy

- Fundamental quantity for nuclear structure at finite temperature
- Essential for low-energy nuclear reaction rates
- Essential for Weak-response at thermal equilibrium

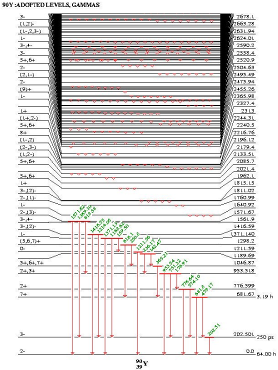

Back-shifted Bethe Formula

$$\rho(E_x) = \frac{1}{\sqrt{2\pi}\sigma}\frac{\sqrt{\pi}}{12}a^{-1/4}(E_x-\Delta)^{-5/4}e^{2\sqrt{a(E_x-\Delta)}}$$

Pairing and shell effects are simulated by a constant shift Δ of the excitation energy.
The parameters a and Δ are determined from data or systematics.

Typically: $a \approx \frac{A}{6} \sim \frac{A}{10}$ $[\mathrm{MeV}^{-1}]$ ($a \approx \frac{A}{15}$ for Fermi gas)
$\Delta_{even-even} = \frac{12}{\sqrt{A}}$, $\Delta_{odd} = 0$, $\Delta_{odd-odd} = -\frac{12}{\sqrt{A}}$

In principle, both a and Δ are not only nucleus dependent but also energy dependent.

Nuclear Level Densities

Mass Dependence of a and Δ

Determination of parameters by fitting SMMC results to the BBF:

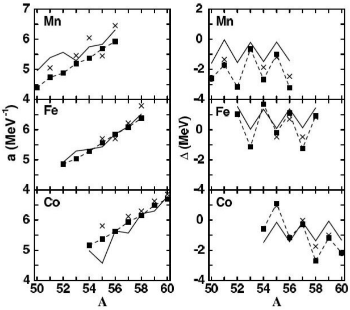

Observe the smooth variation in a, while Δ exhibits odd-even staggering.

Y.Alhassid, nucl-th/0604069, 2006

SMMC Level Densities

$$E(\beta) = \frac{\mathrm{Tr}[He^{-\beta H}]}{\mathrm{Tr}[e^{-\beta H}]} = \frac{\int \mathrm{d}E\, e^{-\beta E} E\rho(E)}{Z(\beta)}$$

$Z(\beta)$: partition function

$$\ln\left[\frac{Z(\beta)}{Z(0)}\right] = -\int_0^{\beta} \mathrm{d}\beta'\, E(\beta')$$

$Z(0)$: total number of states

In the saddle-point approximation,

$$\rho(E) = \frac{e^{\beta E + \ln Z(\beta)}}{\sqrt{-2\pi \frac{\mathrm{d}E(\beta)}{\mathrm{d}\beta}}}$$

where $\beta = \beta(E)$ is the inverse of $E = E(\beta)$.

Nuclear Level Density

What about energy dependence of Δ?

- The BBF, as we have seen, employs a constant Δ to account for important pairing correlations
- However, with increasing excitation energy these correlations must be weakened.
- Ignatyuk introduced energy dependent shifts into the Fermi Gas formula.
- Can the enerrgy dependence of Δ be related to the energy dependence of the pairing correlations?

Nuclear Level Density
Effect of Pairing Component of the Interaction

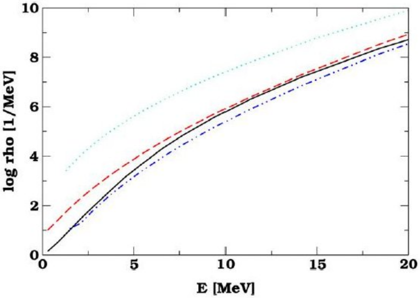

SMMC level density for ^{72}Ge as a function of energy.

K. Langanke, Nucl. Phys. A, 2006.

Nuclear Level Density

Effect of Pairing Component of the Interaction

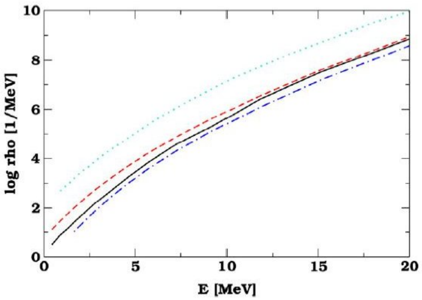

SMMC level density for ^{80}Zr as a function of energy.

K. Langanke, Nucl. Phys. A, 2006.

Nuclear Level Density

Effect of Pairing Component of the Interaction

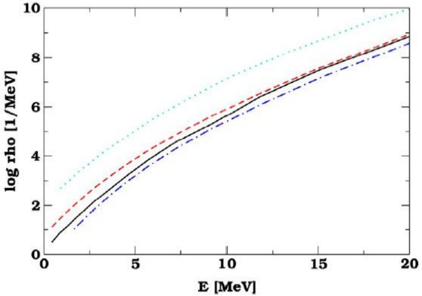

SMMC level density for ^{80}Zr as a function of energy.

Observe the difference with the case before!

Effects of deformation??

K. Langanke, Nucl. Phys. A, 2006.

Nuclear Level Density

Effect of Pairing Component of the Interaction

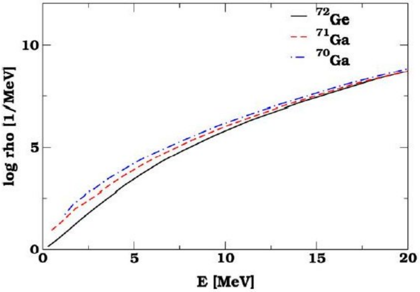

At moderate energies, pairing correlations which are important at low energies are no longer important!

K. Langanke, Nucl. Phys. A, 2006.

Parity and Spin Dependence of the Level Density

Calculation of statistical nuclear reaction rates requires the knowledge of spin and parity-projected distribution of the nuclear energy levels.

Empirical approach:

$$\rho_{J\pi}(E_x) = \frac{1}{2}\mathcal{F}_J(E_x)\rho(E_x)$$

Parity and Spin Dependence of the Level Density

Calculation of statistical nuclear reaction rates requires the knowledge of spin and parity-projected distribution of the nuclear energy levels.

Empirical approach:

$$\rho_{J\pi}(E_x) = \frac{1}{2}\mathcal{F}_J(E_x)\rho(E_x)$$

Parity and Spin Dependence of the Level Density

Calculation of statistical nuclear reaction rates requires the knowledge of spin and parity-projected distribution of the nuclear energy levels.

Empirical approach:

$$\rho_{J\pi}(E_x) = \frac{1}{2}\mathcal{F}_J(E_x)\rho(E_x)$$

Parity and Spin Dependence of the Level Density

Calculation of statistical nuclear reaction rates requires the knowledge of spin and parity-projected distribution of the nuclear energy levels.

Empirical approach:

$$\rho_{J\pi}(E_x) = \frac{1}{2}\mathcal{F}_J(E_x)\rho(E_x)$$

where

$$\mathcal{F}_J(E_x) = \frac{2J+1}{2\sigma^2} e^{\frac{-J(J+1)}{2\sigma^2}}$$

$$\sigma^2 = \frac{\Theta_{\rm rigid}}{\hbar^2}\sqrt{\frac{E_x}{a}} \text{ and } \Theta_{\rm rigid} = \frac{2}{5} m_u A R^2$$

Assumptions:

uncorrelated, randomly coupled single-particle spins and equilibration of opposite-parity states are assumed

SMMC Level Densities: Partial Densities

Let Q be a set of quantum numbers we would like to project out.

$$Y_Q(\beta) = \frac{Z_Q(\beta)}{Z(\beta)} = \frac{\mathrm{Tr}[\hat{P}_Q e^{-\beta H}]}{\mathrm{Tr}[e^{-\beta H}]}, \qquad \therefore \qquad \sum_Q Y_Q(\beta) = 1$$

Energy of excitations with good quantum numbers Q:

$$E_Q(\beta) = -\frac{d\ln Y_Q(\beta)}{d\beta} + E(\beta)$$

Corresponding partial level density follows as

$$\rho_Q(E_Q) = \frac{e^{\beta E_Q + \ln Z_Q(\beta)}}{\sqrt{-2\pi \frac{\mathrm{d}E_Q(\beta)}{\mathrm{d}\beta}}}$$

where $\beta = \beta(E_Q)$ is the inverse of $E_Q = E_Q(\beta)$.

SMMC Level Densities: Partial Densities

Let Q be a set of quantum numbers we would like to project out.

$$Y_Q(\beta) = \frac{Z_Q(\beta)}{Z(\beta)} = \frac{\mathrm{Tr}[\hat{P}_Q e^{-\beta H}]}{\mathrm{Tr}[e^{-\beta H}]}, \qquad \therefore \qquad \sum_Q Y_Q(\beta) = 1$$

Energy of excitations with good quantum numbers Q:

$$E_Q(\beta) = -\frac{d \ln Y_Q(\beta)}{d\beta} + E(\beta)$$

Corresponding partial level density follows as

$$\rho_Q(E_Q) = \frac{e^{\beta E_Q + \ln Z_Q(\beta)}}{\sqrt{-2\pi \frac{\mathrm{d}E_Q(\beta)}{\mathrm{d}\beta}}}$$

where $\beta = \beta(E_Q)$ is the inverse of $E_Q = E_Q(\beta)$.

SMMC Level Densities: Parity Projection¶

Projection onto positive (negative) parity states is carried out by

$$\hat{P}_\pi = \frac{1}{2}(1 + \pi\hat{P})$$

where $\pi = \pm$ and $\hat{P}$=parity operator

In the Hubbard-Stratonovich representation

$$\frac{Z_\pi(\beta)}{Z(\beta)} = \frac{\mathrm{Tr}\left[\hat{P}_\pi e^{-\beta\hat{H}}\right]}{\mathrm{Tr}e^{-\beta\hat{H}}} = \frac{1}{2}\frac{\langle(1 + \pi\frac{\mathrm{Tr}[\hat{P}\hat{U}_\sigma]}{\mathrm{Tr}\hat{U}_\sigma})\Phi_\sigma\rangle_W}{\langle\Phi_\sigma\rangle_W}$$

Grand-canonical trace $\mathrm{Tr}[\hat{P}\hat{U}_\sigma] = \det(1 + \mathbf{P}\mathbf{U}_\sigma)$
where $\mathbf{P}$ is diagonal with matrix elements $(-1)^{l_i}$.

¶ H. Nakada and Y. Alhassid, Phys. Rev. Lett. **79**, 2939 (1997)

Parity-projected SMMC Level Densities for fp-shell Nuclei

Even-even case

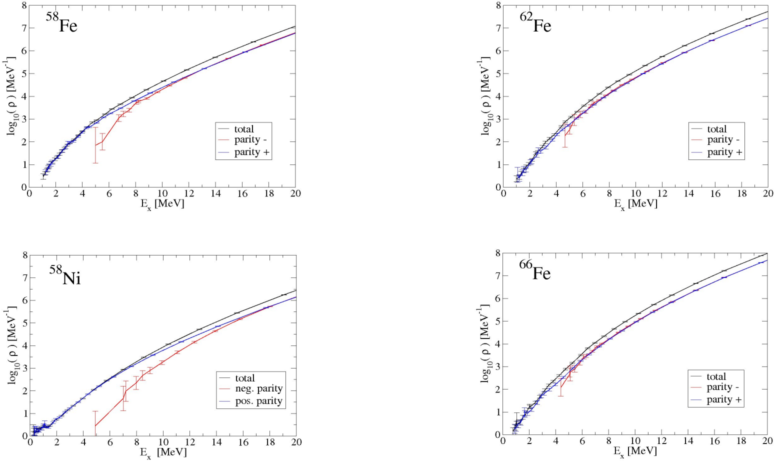

C. Ö., K. Langanke, G. Martinez-Pinedo, D.J. Dean, Phys. Rev. C. **75**,064307,2007.

Parity-projected SMMC Level Densities for fp-shell Nuclei
Interplay between shell structure and pair breaking

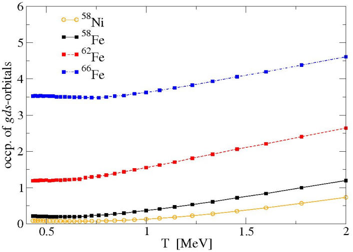

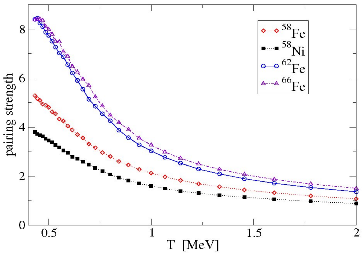

To make negative parity states:
Is it just the occupation of $g_{9/2}$ that matters?

C. Ö., K. Langanke, G. Martinez-Pinedo, D.J. Dean, Phys. Rev. C. **75**,064307,2007.

Parity-projected SMMC Level Densities for fp-shell Nuclei
Interplay between shell structure and pair breaking

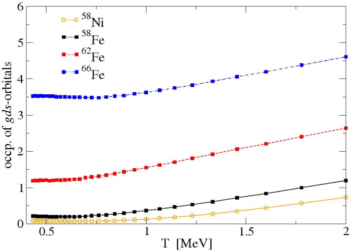

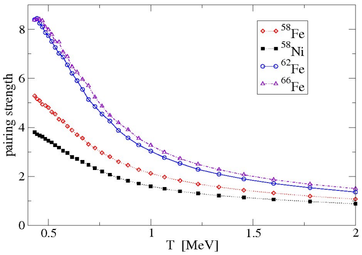

To make negative parity states:
Is it just the occupation of $g_{9/2}$ that matters?
Strong pairing correlations have to be overcome as well!

C. Ö., K. Langanke, G. Martinez-Pinedo, D.J. Dean, Phys. Rev. C. **75**,064307,2007.

Parity-projected SMMC Level Densities for fp-shell Nuclei
Odd-A case

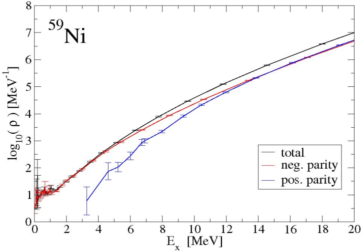

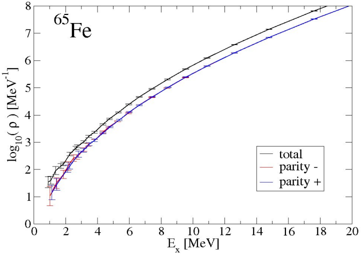

Due to the unpaired nucleon, equilibration of positive and negative parity level level densities is achieved at lower excitation energies compared to the even-even case.

C. Ö., K. Langanke, G. Martinez-Pinedo, D.J. Dean, Phys. Rev. C. **75**,064307,2007.

Nuclear Level Densities
Summary and Outlook

Nuclear Level Densities

Summary and Outlook

- For even-even nuclei, low energy regime is dominated by pairing. Positive-parity level density dominates in this regime.

Nuclear Level Densities
Summary and Outlook

- For even-even nuclei, low energy regime is dominated by pairing. Positive-parity level density dominates in this regime.
- Negative-parity level density is moderated strongly by the single-particle structure.

Nuclear Level Densities

Summary and Outlook

- For even-even nuclei, low energy regime is dominated by pairing. Positive-parity level density dominates in this regime.
- Negative-parity level density is moderated strongly by the single-particle structure.
- In the odd-A case, positive and negative-level densities balance out at lower excitation energies due to the unpaired nucleon in the odd-A nuclei.

SMMC Level Densities: Spin Projection‡

M- and J-projected partition functions are defined as

$$Z_M(\beta) = \mathrm{Tr}_M e^{-\beta H} = \sum_{\alpha, J\geq|M|} \langle \alpha J M | e^{-\beta H} | \alpha J M \rangle = \sum_{\alpha, J\geq|M|} e^{-\beta E_{\alpha,J}}$$

$$Z_J(\beta) = \mathrm{Tr}_J e^{-\beta H} = \sum_{\alpha} \langle \alpha J M | e^{-\beta H} | \alpha J M \rangle = \sum_{\alpha} e^{-\beta E_{\alpha,J}}$$

In general, explicit J-projection is computationally very costly!
However,
Since $e^{-\beta H}$ is a *scalar* operator, one can instead use

$$\mathrm{Tr}_J e^{-\beta H} = \mathrm{Tr}_{M=J} e^{-\beta H} - \mathrm{Tr}_{M=J+1} e^{-\beta H}$$

‡ Y. Alhassid, S. Liu and H. Nakada, nucl-th/0607062

SMMC Level Densities: Spin Projection

Projection onto M-states

$$\hat{P}_M = \frac{1}{2J_s + 1} \sum_{k=-J_s}^{J_s} e^{i\phi_k(\hat{J}_z - M)}$$

where J_s=maximal many-body spin in model space and $\phi_k = \frac{2\pi k}{2J_s+1}$ where $k = -J_s, \ldots, J_s$

In the Hubbard-Stratonovich representation

$$\frac{Z_J(\beta)}{Z(\beta)} = \frac{\mathrm{Tr}\left[\hat{P}_{M=J} e^{-\beta\hat{H}}\right] - \mathrm{Tr}\left[\hat{P}_{M=J+1} e^{-\beta\hat{H}}\right]}{\mathrm{Tr} e^{-\beta\hat{H}}}$$

$$= \frac{\langle (\frac{\mathrm{Tr}_{M=J}[\hat{U}_\sigma]}{\mathrm{Tr}\hat{U}_\sigma} - \frac{\mathrm{Tr}_{M=J+1}[\hat{U}_\sigma]}{\mathrm{Tr}\hat{U}_\sigma}) \Phi_\sigma \rangle_W}{\langle \Phi_\sigma \rangle_W}$$

Spin Distribution of Nuclear Level Densities

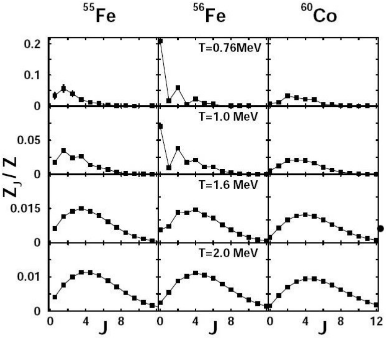

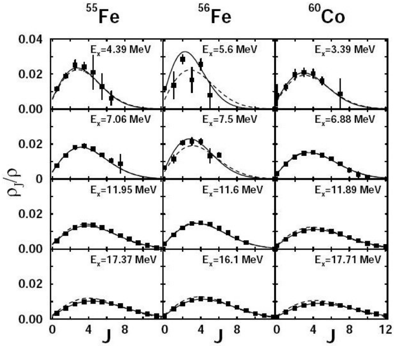

Y. Alhassid, S. Liu and H. Nakada, nucl-th/0607062.

Spin Distribution of Nuclear Level Densities

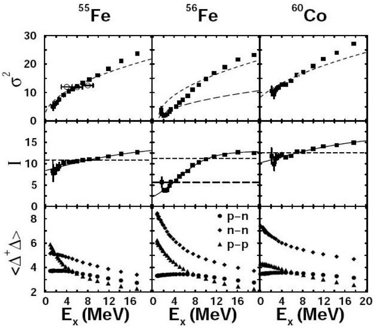

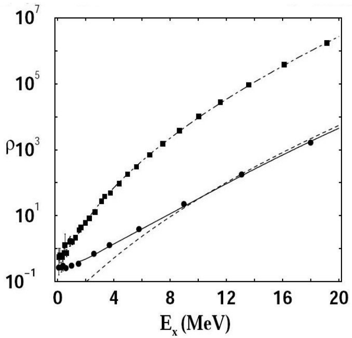

Total and $J = 0$ level densities for ^{56}Fe

$$\sigma^2 = \frac{IT}{\hbar^2} \longrightarrow I(E_x)$$

Energy dependence of moment of inertia

Spin Distribution of Nuclear Level Densities

- little is known about the spin-cutoff parameter experimentally

  SMMC results show that

- spin-cutoff model does a good job for intermediate and high energies
- moment of inertia close to rigid-body value at intermediate and high energies.
- spin cut-off model fails to explain odd-even staggering observed in the even-even nucleus ^{56}Fe for lower values of E_x
- moment of inertia decreases monotonically as E_x become smaller, this suppression is stronger in even-even nucleus ^{56}Fe
- this suppression is correlated with rapid increase in pairing $\longrightarrow$ *thermal signature of pairing phase transition*

Spin and Parity Resolved Level Densities

Level densities $J^\pi = 2^+$ and 2^- extracted from high-resolution $E2$ and $M2$ giant resonances compared to HFB and SMMC calculations.

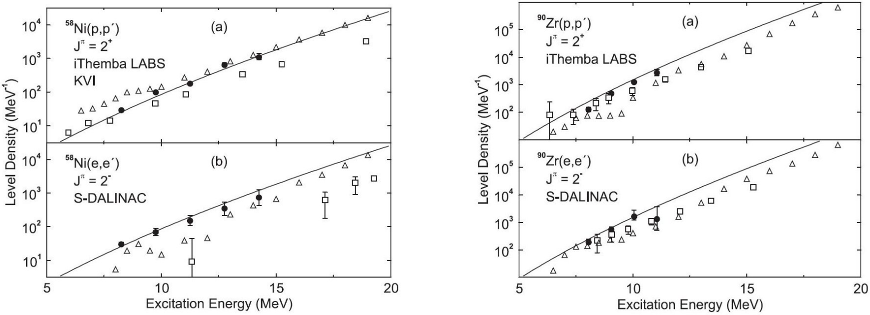

Y. Kalmykov, C. Ö., K. Langanke, G. Martinez-Pinedo, P. von Neumann-Cosel and A.Richter, submitted to PRL.

Spin and Parity Resolved Level Densities

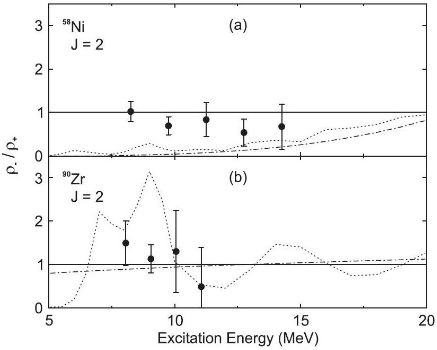

Experiment: no parity dependence

Y. Kalmykov, C. Ö., K. Langanke, G. Martinez-Pinedo, P. von Neumann-Cosel and A.Richter, submitted to PRL.

Spin and Parity Resolved Level Densities

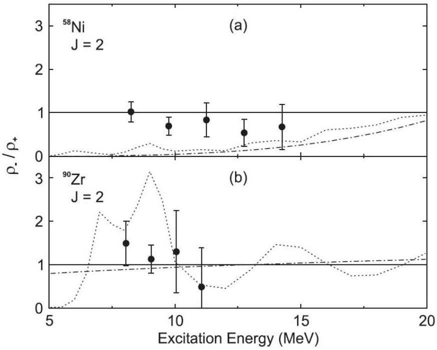

Experiment: no parity dependence

SMMC: neglected core excitations in ^{58}Ni ???

Y. Kalmykov, C. Ö., K. Langanke, G. Martinez-Pinedo, P. von Neumann-Cosel and A.Richter, submitted to PRL.

Spin and Parity Resolved Level Densities

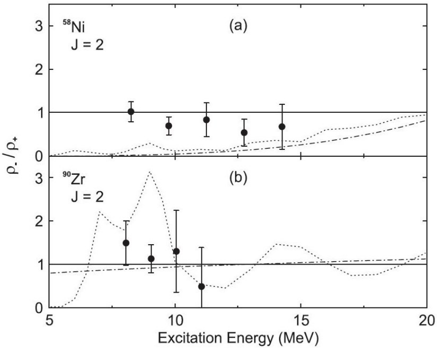

Experiment: no parity dependence

SMMC: neglected core excitations in ^{58}Ni ??? ($\longrightarrow$ more work needed)

Y. Kalmykov, C. Ö., K. Langanke, G. Martinez-Pinedo, P. von Neumann-Cosel and A.Richter, submitted to PRL.

Distribution of Spin and Parity Resolved Level Densities

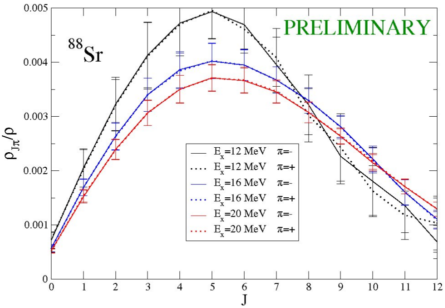

Spin distribution of level densities do not discriminate positive or negative parities at the energies considered.
What happens at lower energies ?

C.Ö, K. Langanke, *work in progress*

SMMC Level Densities

Extending the Theory to Higher Temperatures

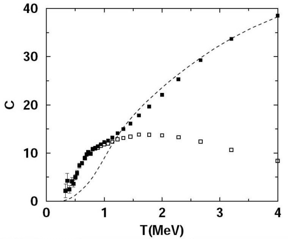

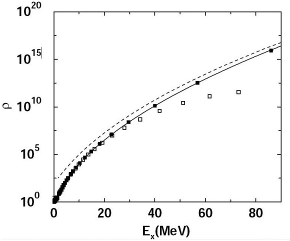

Specific heat and level density for ^{56}Fe. (SMMC calc. in $fpg_{9/2}$ space.)

$$\ln Z_{sp}^{GC} = \sum_{lj}(2j+1)\left\{\sum_{n}\ln[1+e^{-\beta(\epsilon_{nlj}-\mu)}] + \int_0^\infty \mathrm{d}\epsilon\, \delta\rho \ln[1+e^{-\beta(\epsilon_{nlj}-\mu)}]\right\}$$

$$\ln Z_N \approx \ln Z^{GC} - \beta\mu N - \tfrac{1}{2}\ln(2\pi\langle(\Delta N)^2\rangle)$$

$$\ln Z_\nu = \ln Z_{\nu,tr} + \ln Z_{sp} - \ln Z_{sp,tr}$$

Y. Alhassid, G.F. Bertsch, and L. Fang, Phys. Rev. **C68** 044322, 2003.

SMMCpn and Applications to Zr and Mo Isotope Chains

Relaxing the Isospin Symmetry
Motivation

Relaxing the isospin symmetry enables one to treat Hamiltonians built on different proton and neutron model spaces.

Relaxing the Isospin Symmetry

Motivation

Relaxing the isospin symmetry enables one to treat Hamiltonians built on different proton and neutron model spaces.

A typical two-body term $\hat{H}_2 = \sum_\alpha V_\alpha \hat{O}_\alpha^2$ contains $\hat{O}_\alpha = \sum C_{ij}^\alpha a_i^\dagger a_j$

Relaxing the Isospin Symmetry
Motivation

Relaxing the isospin symmetry enables one to treat Hamiltonians built on different proton and neutron model spaces.

A typical two-body term $\hat{H}_2 = \sum_\alpha V_\alpha \hat{O}_\alpha^2$ contains $\hat{O}_\alpha = \sum C_{ij}^\alpha a_i^\dagger a_j$

But

Relaxing the Isospin Symmetry
Motivation

Relaxing the isospin symmetry enables one to treat Hamiltonians built on different proton and neutron model spaces.

A typical two-body term $\hat{H}_2 = \sum_\alpha V_\alpha \hat{\mathcal{O}}_\alpha^2$ contains $\hat{\mathcal{O}}_\alpha = \sum C_{ij}^\alpha a_i^\dagger a_j$

But

$a_p^\dagger a_n$ or $a_n^\dagger a_p$ terms in $\hat{\mathcal{O}}_\alpha = \sum C_{ij}^\alpha a_i^\dagger a_j \longrightarrow Z$ and N fluctuates:

Relaxing the Isospin Symmetry
Motivation

Relaxing the isospin symmetry enables one to treat Hamiltonians built on different proton and neutron model spaces.

A typical two-body term $\hat{H}_2 = \sum_\alpha V_\alpha \hat{\mathcal{O}}_\alpha^2$ contains $\hat{\mathcal{O}}_\alpha = \sum C_{ij}^\alpha a_i^\dagger a_j$

But

$a_p^\dagger a_n$ or $a_n^\dagger a_p$ terms in $\hat{\mathcal{O}}_\alpha = \sum C_{ij}^\alpha a_i^\dagger a_j \longrightarrow Z$ and N fluctuates:

$$e^{-\beta \hat{\mathcal{O}}_\alpha} |\mathrm{SD}\rangle_{Z,N} = |\mathrm{SD}'\rangle_{Z',N'}$$

Relaxing the Isospin Symmetry
Tz-projection

$(Z, N) \Longleftrightarrow (A, T_z)$ must be fixed for the nucleus of interest:

Relaxing the Isospin Symmetry
Tz-projection

$(Z, N) \Longleftrightarrow (A, T_z)$ must be fixed for the nucleus of interest:

$\hat{P}_A = \int_0^{2\pi} \frac{d\phi}{2\pi} e^{-i\phi A} e^{i\phi \hat{N}}$ (Number projection)

$\hat{P}_{T_z} = \int_0^{2\pi} \frac{d\theta}{2\pi} e^{-i\theta T_z} e^{i\theta \hat{T}_z}$ (T_z-projection)

Relaxing the Isospin Symmetry
Tz-projection

$(Z,N) \Longleftrightarrow (A,T_z)$ must be fixed for the nucleus of interest:

$\hat{P}_A = \int_0^{2\pi} \frac{d\phi}{2\pi} e^{-i\phi A} e^{i\phi \hat{N}}$ (Number projection)

$\hat{P}_{T_z} = \int_0^{2\pi} \frac{d\theta}{2\pi} e^{-i\theta T_z} e^{i\theta \hat{T}_z}$ (T_z-projection)

$$\mathrm{Tr}\hat{U}_\sigma = \det(\mathbf{1}+\mathbf{U}) \longrightarrow \int_0^{2\pi} \frac{d\phi}{2\pi} \int_0^{2\pi} \frac{d\theta}{2\pi} e^{-i\phi A} e^{-i\theta T_z} \det(1 + e^{i\phi} e^{i\theta \mathbf{T_z}} \mathbf{U}_\sigma)$$

Applications to $^{90-104}$Zr and $^{92-106}$Mo Isotope Chains

- Region with very large deformations
- Abrupt onset of shape transitions:

$$^{90}\mathrm{Zr},\ ^{96}\mathrm{Zr}\ (\sim \text{spherical}) \longrightarrow\ ^{100-104}\mathrm{Zr}\ (\text{well-deformed})$$

We performed our calculations on a model space containing
$1p_{1/2}, 0g_{9/2}$ (proton)
$1d_{5/2}, 2s_{1/2}, 1d_{3/2}, 0g_{7/2}, 0h_{11/2}$ (neutron)
orbitals on the ^{88}Sr core.

Ground-state energies

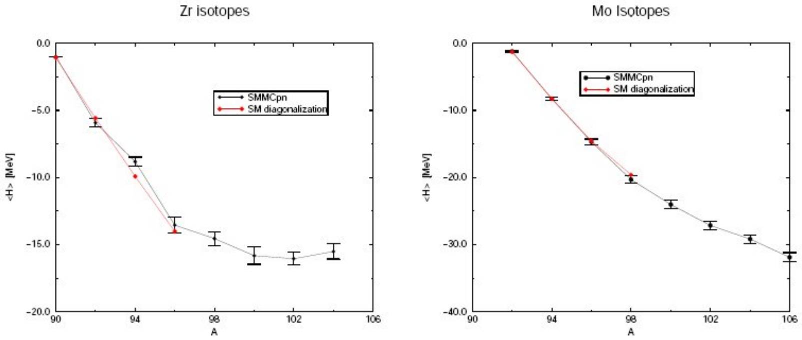

C. Ö., D.J. Dean, Phys.Rev. **C73** 014302,2006.

Binding energies relative to ^{88}Sr

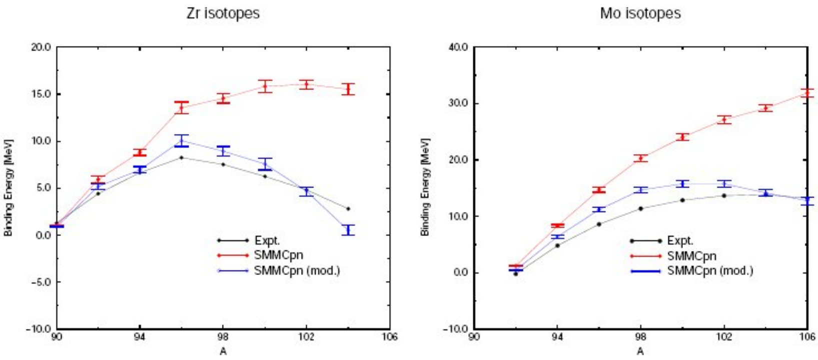

C. Ö., D.J. Dean, Phys.Rev. **C73** 014302,2006.

SMMCpn applied on Zr and Mo isotope chains

Binding Energies

Results show overbinding!
A typical related to the methods used in obtaining effective interactions from meson theory.

$$\Downarrow$$

We make a global monopole correction (due to Zuker):

$V_J^{\mathrm{mod}}(ab,ab) = V_J(ab,ab) + W\frac{n(n-1)}{2}$

where W is adjusted to reproduce experimental values, $W = -125keV$.
(Note that this procedure would not affect excitation spectrum)

Applications on Zr and Mo isotopes

B(E2) strength and Pairing Correlations

- Since the 2_1^+ state is expected to absorb most of the total $B(E2)$ strength, the latter can be used as a measure of the $0_1^+ - 2_1^+$ spacing, which should reflect a strong change with the shape transitions.
  $\hat{Q}_{p(n)} = \sum_i r_i^2 Y_2(\theta_i, \phi_i)$
- Pairing correlations among like nucleons is known to be important for the ground state properties of the even-even nuclei. These correlations are expected to be quenched along the Zr and Mo isotope chains as the transition from spherical to well-deformed shapes becomes more pronounced.

B(E2) strengths

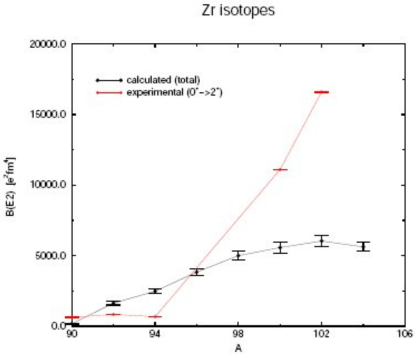

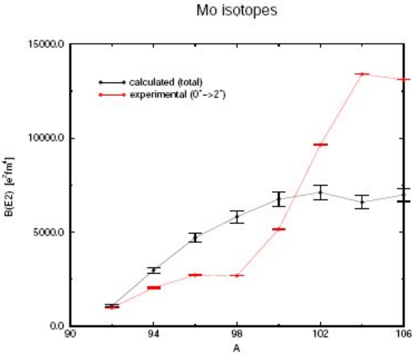

C. Ö., D.J. Dean, Phys.Rev. **C73** 014302,2006.

BCS-like pairing correlations

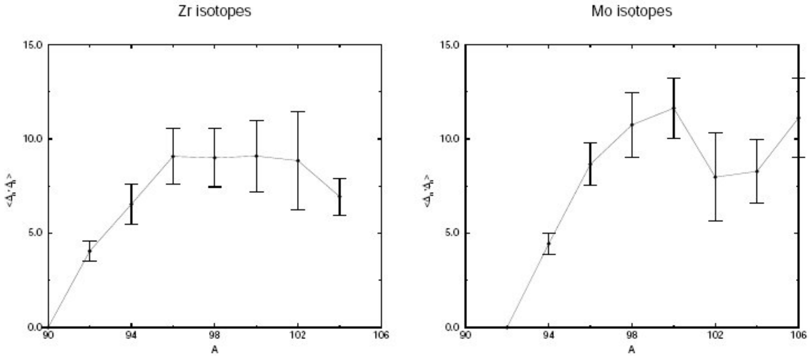

C. Ö., D.J. Dean, Phys.Rev. **C73** 014302,2006.

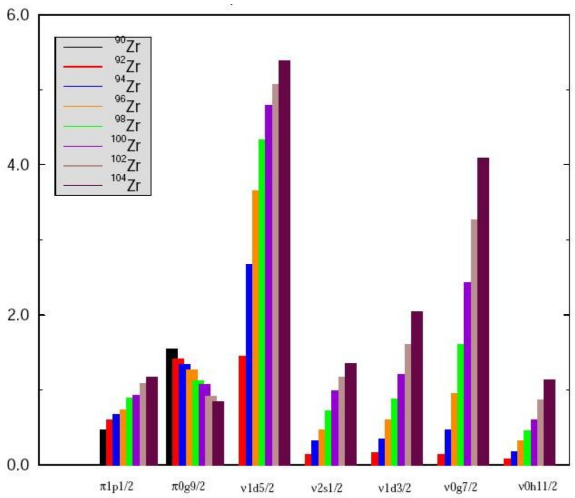

C. Ö., D.J. Dean, Phys.Rev. **C73** 014302,2006.

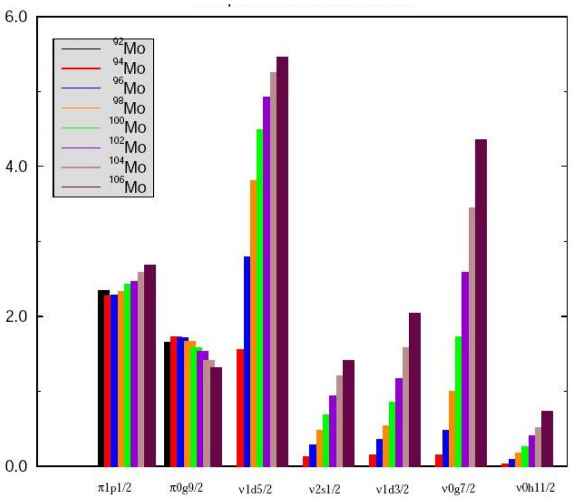

C. Ö., D.J. Dean, Phys.Rev. **C73** 014302,2006.

Summary and Outlook

- First novel applications of the *SMMCpn* code

Summary and Outlook

- First novel applications of the *SMMCpn* code
- Reproduced ground-state energies calculated by exact diagonalization.

Summary and Outlook

- First novel applications of the *SMMCpn* code
- Reproduced ground-state energies calculated by exact diagonalization.
- To reproduce nuclear deformations in the mass region probably requires an extended model space. Further work needs to be done in this mass region.

Electron Capture and β-decay Rates

Electron Capture and β-decay Rates

Late stages of massive stars lifetime are a playground for weak-interaction processes that play an important role in the fate of the star.

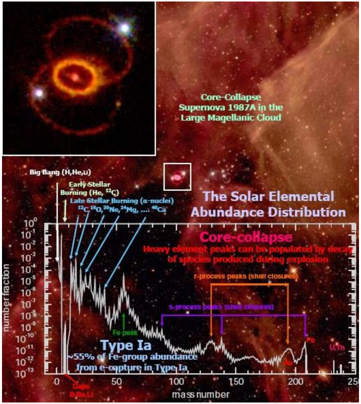

Picture from G.W. Hitt and H. Schatz

Isotopic composition in Type Ia supernoavae is controlled by e^--capture

In the core-collapse supernovae pre-collapse conditions are strongly dependent on e^--capture Competition between e^--capture and β-decay rates is very important.

Both e^--capture and β-decay cause a leak of energy and entropy through emission of neutrinos (for $\rho \lesssim 10^{11}$ g cm^{-3})

Weak-interaction rates

SMMC has been the naturally suitable method for the determination of pre-collapse supernova weak-interaction rates. Because

- Large dimensions of the problem ($fp - gds$ shells)
- Requirement of finite temperature treatment due to astrophysical conditions

Some recent calculations are

for Neutron-rich Ge isotopes:

K. Langanke and G. Martinez-Pinedo, At. Data. Nucl. Data Tables **79** 1, 2001.

for $A = 65 - 112$ nuclei:

K. Langanke and G. Martinez-Pinedo, Rev. Mod. Phys. **75** 819, 2003.

Gamow-Teller Transitions

β-decay vs. Electron capture

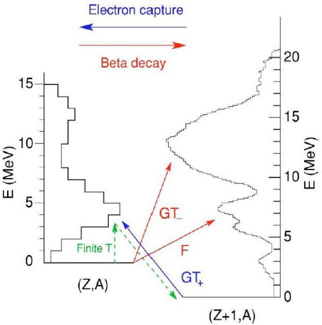

β-decay:

$$A(Z,N) \longrightarrow A(Z+1,N-1) + e^- + \bar{\nu}_e$$

Electron capture:

$$A(Z,N) + e^- \longrightarrow A(Z-1,N+1) + \nu_e$$

$$Q_\beta = M_i - M_f + E_i - E_f$$

Gamow-Teller Transitions

Why so important?

- Highly energetic electrons in the fully ionized stellar environment can be captured to GT resonances in the decaying nucleus.
- Presence of degenerate electron gas may block the phase space of the electron from beta decaying nucleus
- Finite temperature combined with GT transitions to low-lying states in daughter nucleus may enhance phase space and therefore beta-decay rates

Gamow-Teller Transitions

IPM vs. SM at Finite T

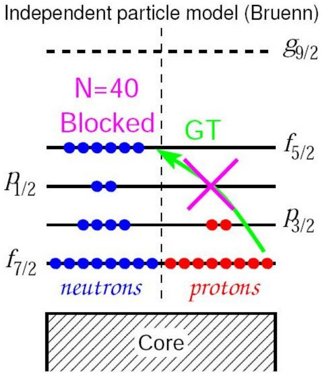

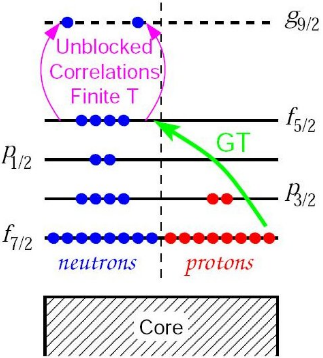

Weak Rates for nuclei with A=65–112 computed using the Shell Model Monte Carlo plus RPA approach

From K. Langanke

Electron Capture Rates

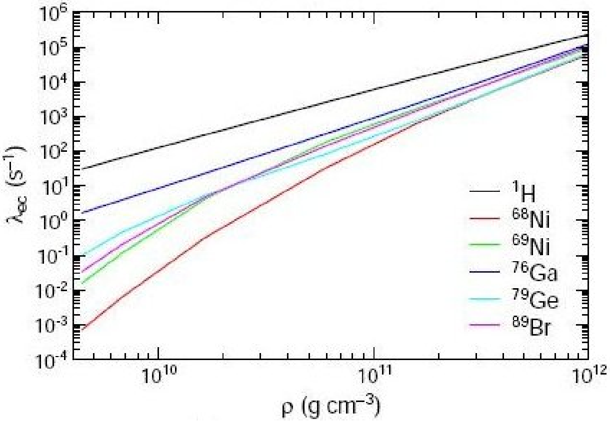

From K. Langanke

Electron Capture Rates

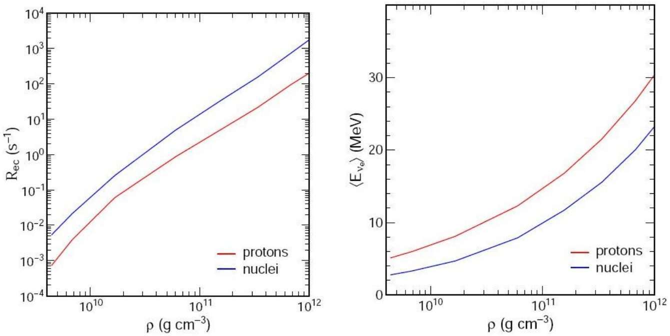

Electron capture on nuclei dominates over capture on protons

From K. Langanke

Electron Capture Rates

- Previously neglected e^--capture on nuclei $N > 40$, $Z < 40$ were shown to be very important.
- Correlations with finite temperature effects unblock the GT transitions.
- SMMC (for T-dependent occ. numbers) + RPA (for capture rates) have shown that capture on nuclei dominates capture on protons.
- Although $\langle E_{\nu_e} \rangle$ is less for nuclei than for protons ($\approx 40 - 60\%$), contributions from nuclei cause significant effect since neutrino-matter interactions scale with the square of the neutrino energy.

Outlook

In the next decades SMMC will continue to be the wavefront of the large-scale shell model calculations, with the alleviation of the sign problem its impact will probably become even greater. Efforts will focus particularly on

- Extending shell model calculations to regions away from the line of stability
- Establishing connections with self-consistent mean-field theory and shell model;
  Derivation of a universal Hamiltonian
- Develop a global theory of nuclear level densities